NUWC-NPT Technical Report 11,280
10 April 2001

Saddlepoint Approximations for Various Statistics of Dependent, Non-Gaussian Random Variables: Applications to the Maximum Variate and the Range Variate

Albert H. Nuttall
Surface Undersea Warfare Department

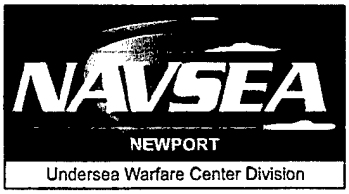

Naval Undersea Warfare Center Division
Newport, Rhode Island

PREFACE

The work described in this report was funded by Project No. A101401, "Automatic Signal Classification," principal investigator Stephen G. Greineder (Code 2121). The sponsoring activity is the Office of Naval Research, program manager John Tague (Code 321US).

The technical reviewer for this report was Richard A. Katz (Code 3113).

Reviewed and Approved: 10 April 2001

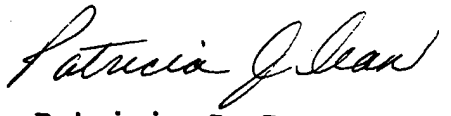

Patricia J. Dean
Director, Surface Undersea Warfare

REPORT DOCUMENTATION PAGE

Form Approved
OMB No. 0704-0188

1. AGENCY USE ONLY *(Leave blank)*	2. REPORT DATE	3. REPORT TYPE AND DATES COVERED
	10 April 2001	

4. TITLE AND SUBTITLE

Saddlepoint Approximations for Various Statistics of Dependent, Non-Gaussian Random Variables: Applications to the Maximum Variate and the Range Variate

5. FUNDING NUMBERS

6. AUTHOR(S)

Albert H. Nuttall

7. PERFORMING ORGANIZATION NAME(S) AND ADDRESS(ES)

Naval Undersea Warfare Center Division
1176 Howell Street
Newport, RI 841-1708

8. PERFORMING ORGANIZATION REPORT NUMBER

TR, 11,280

9. SPONSORING/MONITORING AGENCY NAME(S) AND ADDRESS(ES)

Office of Naval Research (321US)
Ballston Centre Tower One
800 North Quincy Street
Arlington, VA 22217-5660

10. SPONSORING/MONITORING AGENCY REPORT NUMBER

11. SUPPLEMENTARY NOTES

12a. DISTRIBUTION/AVAILABILITY STATEMENT

Approved for public release; distribution is unlimited.

12b. DISTRIBUTION CODE

13. ABSTRACT (Maximum 200 words)

The determination of the statistics of a set of random variables (RVs) is frequently achieved by assuming the RVs to be joint Gaussian or to be statistically independent of each other. Although this assumption greatly simplifies the analysis, it can lead to very misleading probability measures, especially on the tails of the distributions, where the exact details of the particular RVs can be important.

This report presents a new method for deriving saddlepoint approximations (SPAs) for a number of very useful statistics of a general set of M dependent RVs, including the joint moments, the joint cumulative distribution function (CDF), the joint exceedance distribution function (EDF), and the joint probability density function (PDF). In particular, application to the maximum RV of a set of M dependent non-Gaussian RVs will be thoroughly investigated for two different examples. Also, the statistics of the range variate (maximum - minimum) are determined for the same two examples.

The calculation of these M-dimensional statistics sometimes requires that multiple M-dimensional SPs be determined in order to evaluate an EDF or PDF at a single point in probability space. Also, the storage requirements and/or execution times can rapidly grow unmanageable as the number of dimensions, M, increases. Finally, care must be taken to ensure that the SP is located in the correct region of M-dimensional space; this allowed region of analyticity varies with the particular statistic under investigation.

14. SUBJECT TERMS			15. NUMBER OF PAGES
Dependent Variables	Joint Statistics	Non-Gaussian	83
Range Variate	Maximum Variate		16. PRICE CODE

17. SECURITY CLASSIFICATION OF REPORT	18. SECURITY CLASSIFICATION OF THIS PAGE	19. SECURITY CLASSIFICATION OF ABSTRACT	20. LIMITATION OF ABSTRACT
Unclassified	Unclassified	Unclassified	SAR

TABLE OF CONTENTS

TABLE OF CONTENTS (Cont'd)

LIST OF ILLUSTRATIONS

LIST OF ABBREVIATIONS, ACRONYMS, AND SYMBOLS

a	Average value of y, equations (14) and (18)
a_0	Zeroth-order saddlepoint approximation, equation (55)
a_1	First-order saddlepoint approximation, equation (56)
a_e	Exponential saddlepoint approximation, equation (57)
A	Linear transformation, equations (88) and (90)
ASY	Asymptotic form
C	Contour in M-dimensional λ space, equation (18)
CDF	Joint cumulative distribution function, equation (3)
C_m	m-th Bromwich contour of integration, equation (10)
CGF	Joint cumulant generating function, equation (11)
C_l	Contour which passes left of origin, equation (59)
C_r	Contour which passes right of origin, equation (42)
c_t	First-order correction term, equation (56)
$c_y(y)$	Cumulative distribution of maximum y, equation (58)
$c_z(z)$	Joint cumulative distribution function, equation (3)
det	Determinant, equation (55)
D	Diamond in u space, equation (43)
$\{e_n\}$	Exponential random variables, test example (2)
EDF	Joint exceedance distribution function, equation (4)
E(v)	Expectation of random variable v, equation (9)
ETE	Exponential test example
$e_y(y)$	Exceedance distribution of maximum y, equation (65)
$e_z(z)$	Joint exceedance distribution function, equation (4)
FFT	Fast Fourier transform
g(u)	Nonlinear transformation, equation (12)

LIST OF ABBREVIATIONS, ACRONYMS, AND SYMBOLS (Cont'd)

GHQ	Gauss-Hermite quadrature
GTE	Gaussian test example
H_k	Hypothesis k, k = 0 or 1
max	maximum, equation (86)
min	minimum, equation (86)
M	Number of random variables $\{z_m\}$, equation (1)
MGF	Joint moment generating function, equation (9)
N	Number of exponential variables, test example (2)
$p_{a,b}$	Probability density estimates, equations (82) and (83)
P_d	Probability of detection
PD	Partial derivative, equation (49)
PDF	Joint probability density function, equation (2)
P_f	Probability of false alarm
P_k	Quadrant probabilities, equation (64)
Pr(e)	Probability of event e, equation (3)
$p_y(y)$	Probability density of maximum y, equation (72)
$p_z(z)$	Probability density function value at z, equation (2)
Q_k	Quadrants, equation (64)
Re	Real part
ROA	Region of analyticity, equation (9)
R_μ	Region of real λ where $\mu_z(\lambda)$ exists, equation (9)
RV	Random variable or random vector, equation (1)
s	Vector variable of integration, equation (55)
SIM	Simulation results
SP	Saddlepoint, equation (49)

LIST OF ABBREVIATIONS, ACRONYMS, AND SYMBOLS (Cont'd)

SPA	Saddlepoint approximation, equation (55)
u	Vector $[u_1 \cdots u_M]'$, equation (8)
U(x)	Unit step function, equation (23)
x	N-dimension random vector, equation (86)
y	Random scalar, equations (12) and (58)
y	Ordered random variables, equation (93)
z	Mx1 vector, field point of interest, equation (2)
{z(m)}	Components of vector z, m=1:M, equation (2)
z	Mx1 random vector, equation (1)
{z(m)}	Components of random vector z, m=1:M, equation (1)
α	Nx1 vector argument of $\mu_{\mathbf{x}}$, equation (86)
δ	Delta function, equation (19)
∂	Partial derivative, equation (49)
δ_{jk}	Kronecker delta, equation (62)
$\gamma(\lambda)$	Gamma function, equation (16)
λ	Mx1 vector in MGF domain, equation (9)
$\{\lambda(m)\}$	Components of vector λ, m=1:M, equation (9)
$\hat{\lambda}$	Saddlepoint, equation (49)
$\hat{\lambda}_m$	m-th component of SP vector $\hat{\lambda}$, equation (50)
$\Lambda(\lambda)$	Logarithm of total integrand, equation (48)
$\Lambda_2(m,\underline{m})$	Second-order PDs of $\Lambda(\lambda)$ at SP, equation (51)
Λ_2	MxM matrix of PDs of $\Lambda(\lambda)$ at SP, equation (52)
μ_n	Auxiliary moment generating function, equation (67)
$\mu_{\mathbf{x}}(\alpha)$	Joint moment generating function of **x**, equation (92)

LIST OF ABBREVIATIONS, ACRONYMS, AND SYMBOLS (Cont'd)

$\mu_z(\lambda)$	Joint moment generating function of z, equation (9)
ν_m	Power law parameter, equation (39)
χ_n	Auxiliary cumulant generating function, equation (68)
$\chi_z(\lambda)$	Joint cumulant generating function, equation (11)
' (prime)	Transpose
boldface	Random variable or random vector

SADDLEPOINT APPROXIMATIONS FOR VARIOUS STATISTICS OF DEPENDENT NON-GAUSSIAN RANDOM VARIABLES: APPLICATIONS TO THE MAXIMUM VARIATE AND THE RANGE VARIATE

INTRODUCTION

Evaluation of the joint cumulative distribution function (CDF) or joint exceedance distribution function (EDF) from the corresponding joint probability density function (PDF) is a very difficult task in M dimensions when M is approximately greater than four. Even in the simplest nontrivial case, namely, when the joint PDF is Gaussian with known non-diagonal covariance matrix and mean vector, the required integrals over an M-dimensional subspace are not amenable to numerical integration.

However, a number of probabilistic problems are amenable to the analytic evaluation of the joint moment generating function (MGF) of the M random variables (RVs) of interest, even though the corresponding joint PDF is not available in any useful analytic form (reference 1). In these cases, it would be very useful to have a means for determining the joint CDF, joint EDF, and/or joint moments directly from the M-dimensional joint MGF, without having to bother with the intermediate joint PDF. This report presents just such a technique for accomplishing this goal by extending Parseval's theorem, relating one-dimensional Fourier transforms, to M-dimensional Laplace transforms with movable Bromwich contours.

The additional freedom afforded by moving contours in complex M-dimensional space allows for use of an M-dimensional saddlepoint (SP) of the integrand relating the joint MGF to the statistic(s) of interest. A saddlepoint approximation (SPA) can then be developed about this special point for the desired statistical quantity of interest. Although this procedure requires the numerical determination of an M-dimensional SP, it affords a reasonable practical means for approximately evaluating some joint probabilities and joint moments that have been previously inaccessible. An excellent review of the SP method is given in reference 2, in addition to a thorough bibliography.

The calculation of these M-dimensional statistics is not bought cheaply. It is sometimes required that multiple M-dimensional SPs be determined to evaluate an EDF or PDF at a single point in probability space. Also, the storage requirements and/or execution times can rapidly grow unmanageable as the number of dimensions, M, increases. Finally, care must be taken to ensure that the appropriate SP is located in the correct region of M-dimensional space; this allowed region of analyticity varies with the particular statistic under investigation.

PROBABILITY NOTATION

Random variables will be denoted by **boldface** type. Thus, real random vector (RV) $\mathbf{z}$ is an Mx1 column vector

$$\mathbf{z} = [z_1 \cdots z_M]' \ , \tag{1}$$

with random components $\{z_m\}$, m=1:M, that may be statistically dependent on each other. On the other hand, $z = [z_1 \cdots z_M]'$ is an Mx1 vector of ordinary real variables $\{z_m\}$. The joint PDF of RV $\mathbf{z}$ at argument z is denoted as

$$p_{\mathbf{z}}(z) = p_{\mathbf{z}}(z_1,\ldots,z_M) \ . \tag{2}$$

The corresponding joint CDF of RV $\mathbf{z}$ at argument z is

$$c_{\mathbf{z}}(z) = c_{\mathbf{z}}(z_1,\ldots,z_M) = \int_{-\infty}^{z_1} du_1 \cdots \int_{-\infty}^{z_M} du_M \ p_{\mathbf{z}}(u_1,\ldots,u_M) =$$

$$= \Pr(\mathbf{z}_1 < z_1,\ldots,\mathbf{z}_M < z_M) \ , \tag{3}$$

where Pr(e) is the probability of event e. The corresponding joint EDF of RV $\mathbf{z}$ at argument z is

$$e_{\mathbf{z}}(z) = e_{\mathbf{z}}(z_1,\ldots,z_M) = \int_{z_1}^{\infty} du_1 \cdots \int_{z_M}^{\infty} du_M \ p_{\mathbf{z}}(u_1,\ldots,u_M) =$$

$$= \Pr(\mathbf{z}_1 > z_1,\ldots,\mathbf{z}_M > z_M) \ . \tag{4}$$

It should be noted that $c_{\mathbf{z}}(z) + e_{\mathbf{z}}(z) < 1$, generally, in M dimensions for M > 1.

MIXED PROBABILITY FUNCTIONS

It will be necessary later to introduce and utilize some mixed probability functions. For example, the following quantity is M-1 parts CDF and 1 part EDF:

$$\Pr(\mathbf{z}_1 < z_1, \ldots, \mathbf{z}_{M-1} < z_{M-1}, \mathbf{z}_M > z_M) =$$

$$= \int_{-\infty}^{z_1} du_1 \cdots \int_{-\infty}^{z_{M-1}} du_{M-1} \int_{z_M}^{\infty} du_M \; p_{\mathbf{z}}(u_1, \ldots, u_M) \; . \tag{5}$$

On the other hand, the following quantity is 1 part PDF and M-1 parts CDF:

$$\int_{-\infty}^{z_2} du_2 \cdots \int_{-\infty}^{z_M} du_M \; p_{\mathbf{z}}(z_1, u_2, \ldots, u_M) \; . \tag{6}$$

Finally, although the following quantity is not encountered in this report, it is listed to demonstrate the great generality of the probability procedure to be presented here, namely,

$$\int_{-\infty}^{z_1} du_1 \int_{z_4}^{\infty} du_4 \int_{z_5}^{\infty} du_5 \int_{-\infty}^{z_7} du_7 \int_{-\infty}^{z_9} du_9 \; p_{\mathbf{z}}(u_1, z_2, z_3, u_4, u_5, z_6, u_7, z_8, u_9, z_{10}) \tag{7}$$

is five parts PDF, three parts CDF, and two parts EDF. It should be observed that all of the probabilistic quantities here are special cases of the M-dimensional integral

$$\int du_1 \cdots \int du_M \; p_{\mathbf{z}}(u_1, \ldots, u_M) \; g(u_1, \ldots, u_M) = \int du \; p_{\mathbf{z}}(u) \; g(u). \tag{8}$$

TRANSFORM DOMAIN

The transform domain is denoted in terms of Mx1 complex vector $\lambda = [\lambda_1 \cdots \lambda_M]'$. In particular, the joint MGF $\mu_z(\lambda)$ corresponding to joint PDF $p_z(z)$ is given by expectation

$$\mu_z(\lambda) = E \exp(\lambda' z) = E \exp\left(\sum_{m=1}^{M} \lambda_m z_m\right) =$$

$$= \int dz_1 \cdots \int dz_M \, p_z(z_1,\ldots,z_M) \exp(\lambda' z) \, . \qquad (9)$$

When the imaginary part, λ_i, of vector λ is zero, integral (9) exists for $Re(\lambda) \in R_\mu$, where M-dimensional real region R_μ always includes the origin $\lambda = 0$. It immediately follows from the form of equation (9) that joint MGF $\mu_z(\lambda)$ will exist for <u>all</u> values of vector λ_i when $Re(\lambda) \in R_\mu$. This M-dimensional λ region of definition of joint MGF $\mu_z(\lambda)$ is called the region of analyticity, $ROA(\mu_z)$; that is, $ROA(\mu_z)$ is the M-dimensional set of complex λ values such that $Re(\lambda) \in R_\mu$.

The joint PDF $p_z(z)$ at vector argument z may be obtained from the joint MGF $\mu_z(\lambda)$ by means of M-dimensional inverse Laplace transform

$$p_z(z) = \frac{1}{(i2\pi)^M} \int_{C_1} d\lambda_1 \cdots \int_{C_M} d\lambda_M \, \mu_z(\lambda_1,\ldots,\lambda_M) \exp(-\lambda' z) \, , \qquad (10)$$

where Bromwich contours $\{C_m\}$, m=1:M, initially lie in the $ROA(\mu_z)$. The m-th Bromwich contour C_m parallels the imaginary

axis λ_{mi} and remains in the ROA(μ_z). However, the freedom to move all the contours $\{C_m\}$ within the ROA allows for an advantageous choice of locations, namely, through the M-dimensional real SP of the integrand of equation (10) that lies in ROA(μ_z); see reference 1 for an example.

The corresponding joint cumulant generating function (CGF) of RV z is given by

$$\chi_z(\lambda) = \ln \mu_z(\lambda) \quad \text{for } \lambda \in \text{ROA}(\mu_z) \ . \tag{11}$$

REAL NONLINEAR TRANSFORMATIONS

Suppose random vector $\mathbf{z}$ is subjected to the real nonlinear transformation $g(u) = g(u_1,\ldots,u_M)$ according to

$$\mathbf{y} = g(\mathbf{z}_1,\ldots,\mathbf{z}_M) \ , \tag{12}$$

leading to real scalar RV $\mathbf{y}$. Two examples are

$$\mathbf{y} = \frac{1}{M}\left(\mathbf{z}_1^{\nu} + \cdots + \mathbf{z}_M^{\nu}\right) \quad \text{and} \quad \mathbf{y} = \max(\mathbf{z}_1,\ldots,\mathbf{z}_M) \ . \tag{13}$$

The average value of RV $\mathbf{y}$ in equation (12) is given by

$$a = E(\mathbf{y}) = E\ g(\mathbf{z}_1,\ldots,\mathbf{z}_M) =$$

$$= \int du_1 \cdots \int du_M\ p_{\mathbf{z}}(u_1,\ldots,u_M)\ g(u_1,\ldots,u_M) \ . \tag{14}$$

This is the same M-dimensional integral encountered in equations (5) through (8). However, M-dimensional integral (14) is virtually always too difficult to determine analytically; also, for large M, it is extremely difficult to evaluate numerically due to storage and execution time limitations. Accordingly, an alternative, more useful form for integral (14) will be developed

Substitute expression (10) for joint PDF $p_{\mathbf{z}}$ into equation (14) and interchange the M-dimensional integrals to obtain

$$a = \frac{1}{(i2\pi)^M} \int_{C_1} d\lambda_1 \cdots \int_{C_M} d\lambda_M\ \mu_{\mathbf{z}}(\lambda_1,\ldots,\lambda_M) \times$$

$$\times \int du_1 \cdots \int du_M\ g(u_1,\ldots,u_M)\ \exp(-\lambda' u) \ . \tag{15}$$

The outer integrals in equation (15) require that λ be kept in the ROA of $\mu_z(\lambda)$. At the same time, the inner integrals on u in equation (15), to be denoted by gamma function $\gamma(\lambda)$, will converge only for vector λ within a restricted region of M-dimensional space. That is, gamma function

$$\gamma(\lambda_1,\ldots,\lambda_M) = \int du_1 \cdots \int du_M \; g(u_1,\ldots,u_M) \exp(-\lambda' u) \qquad (16)$$

exists only for $\lambda \in \mathrm{ROA}(\gamma)$. Use of relation (16) in equation (15) yields the alternative expression of interest for average a:

$$a = \frac{1}{(i2\pi)^M} \int_{C_1} d\lambda_1 \cdots \int_{C_M} d\lambda_M \; \mu_z(\lambda_1,\ldots,\lambda_M) \; \gamma(\lambda_1,\ldots,\lambda_M) \; . \qquad (17)$$

In more compact notation, from equations (14) and (17),

$$a = \int du \; p_z(u) \; g(u) = \frac{1}{(i2\pi)^M} \int_C d\lambda \; \mu_z(\lambda) \; \gamma(\lambda) \; , \qquad (18)$$

where M-dimensional contour C must lie in the intersection of the ROAs of $\mu_z(\lambda)$ and $\gamma(\lambda)$; that is, $C \in \mathrm{ROA}(\mu_z,\gamma) \equiv \mathrm{ROA}(\mu_z) \cap \mathrm{ROA}(\gamma)$.

The relation (18) is exact; there are no approximations involved in this identity. However, the M-dimensional integral on λ will generally not be capable of evaluation analytically either; but the fact that the M-dimensional contour C in equation (18) can be moved about in the restricted $\mathrm{ROA}(\mu_z,\gamma)$ affords the chance of developing an SPA for the last term in equation (18) about a SP in this region.

PROS AND CONS OF EQUATION (18)

The first integral in equation (18), I_1, has an immediate physical interpretation as the average of nonlinear transformation g, whereas the second integral in equation (18), I_2, has no direct physical interpretation. Also, it is easy to directly specify nonlinearity g in I_1, whereas gamma function γ in I_2 must be obtained via the M-dimensional Laplace transformation (16).

On the other hand, many probabilistic problems have no convenient expression for the joint PDF p_z, whereas the joint MGF μ_z can sometimes be obtained in closed form; see reference 1, for example, where the joint MGF for M quadratic and linear forms in K dependent Gaussian RVs is derived. Also, whereas development of an SPA for I_1 in equation (18) is difficult due to the discontinuities inherent in typical g functions, the SPA for I_2 in equation (18) can be developed more easily by moving M-dimensional contour C to an appropriate SP in λ space.

The availability of a closed form for joint MGF μ_z, combined with the lack of knowledge of joint PDF p_z, weighs very heavily for form I_2 over I_1 in equation (18). The major drawback with I_2 is in getting the M-dimensional Laplace transform γ of nonlinearity g; however, for an important class of physically meaningful problems, the g function is separable in its arguments $u = [u_1 \cdots u_M]'$, thereby allowing reduction of equation (16) to M one-dimensional Laplace transforms, a very workable approach.

EXAMPLES OF TRANSFORMATION g(u)

Example 1. $g_z(u_1,\ldots,u_M) = \delta(u_1-z_1) \cdots \delta(u_M-z_M)$, (19)

where vector $z = [z_1 \cdots z_M]'$ represents an arbitrary point in real M-dimensional space. Substitution of equation (19) in the left-hand side of equation (18) yields

$$a = \int du\ p_z(u)\ g_z(u) = p_z(z_1,\ldots,z_M) \ , \tag{20}$$

which is simply the joint PDF of RV z at argument z. At the same time, substitution of equation (19) into equation (16) yields

$$\gamma_z(\lambda) = \exp(-\lambda' z) = \exp\left(-\sum_{m=1}^{M} \lambda_m\ z_m\right) \quad \text{for } \underline{\text{any}}\ \{\lambda_m\} \ . \tag{21}$$

That is, the ROA(γ) is infinite for this particular impulsive g example in equation (19); therefore ROA(μ_z,γ) = ROA(μ_z). Use of equation (21) in equation (18) yields the alternative

$$a = \frac{1}{(i2\pi)^M} \int_C d\lambda\ \mu_z(\lambda)\ \exp(-\lambda' z) \ , \tag{22}$$

which is the usual expression (10) for the joint PDF $p_z(z)$.

Nothing new has been learned from this particular example for nonlinearity g. However, the method developed here will be used for all the following examples, without additional explanation. A key point is to note the ROA(γ) when equation (16) is evaluated for the particular g example under consideration. This must be coupled with ROA(μ_z) according to ROA(μ_z,γ) = ROA(μ_z) $\cap$ ROA(γ).

Example 2. $g_z(u_1,\ldots,u_M) = U(z_1-u_1) \cdots U(z_M-u_M)$, (23)

where unit step function U(x) is 1 for x > 0 and is 0 for x < 0. Then, average (14) becomes

$$a = \int_{-\infty}^{z_1} du_1 \cdots \int_{-\infty}^{z_M} du_M \; p_z(u_1,\ldots,u_M) = c_z(z_1,\ldots,z_M) \; , \qquad (24)$$

which is the joint CDF of RV z at argument $z = [z_1 \cdots z_M]'$. The gamma function (16), corresponding to nonlinearity (23), is

$$\gamma_z(\lambda) = \int_{-\infty}^{z_1} du_1 \cdots \int_{-\infty}^{z_M} du_M \; \exp(-\lambda_1 \; u_1 - \cdots - \lambda_M \; u_M) =$$

$$= \frac{\exp(-\lambda_1 \; z_1)}{-\lambda_1} \cdots \frac{\exp(-\lambda_M \; z_M)}{-\lambda_M} = \exp(-\lambda' z) \Big/ \prod_{m=1}^{M} (-\lambda_m) \qquad (25)$$

if $\mathrm{Re}(\lambda_m) < 0$ for m=1:M. Therefore, average

$$a = c_z(z) = \frac{1}{(i2\pi)^M} \int_C d\lambda \; \mu_z(\lambda) \; \exp(-\lambda' z) \Big/ \prod_{m=1}^{M} (-\lambda_m) \; , \qquad (26)$$

provided that the m-th Bromwich contour C_m stays to the <u>left</u> of the origin for m=1:M, and also stays within the ROA of joint MGF $\mu_z(\lambda)$. Relation (26) provides a method for obtaining the joint CDF $c_z(z)$ at arbitrary M-dimensional point z directly from the joint MGF $\mu_z(\lambda)$ without having to calculate or deal with joint PDF $p_z(z)$.

Example 3. $g_z(u_1,\ldots,u_M) = U(u_1-z_1) \cdots U(u_M-z_M)$, (27)

where unit step function U(x) is 1 for x > 0 and is 0 for x < 0. Then, average (14) becomes

$$a = \int_{z_1}^{\infty} du_1 \cdots \int_{z_M}^{\infty} du_M \; p_z(u_1,\ldots,u_M) = e_z(z_1,\ldots,z_M) \; , \qquad (28)$$

which is the joint EDF of RV z at argument $z = [z_1 \cdots z_M]'$. The gamma function (16) corresponding to nonlinearity (27) is

$$\gamma_z(\lambda) = \int_{z_1}^{\infty} du_1 \cdots \int_{z_M}^{\infty} du_M \; \exp(-\lambda_1 u_1 - \cdots - \lambda_M u_M) =$$

$$= \frac{\exp(-\lambda_1 z_1)}{\lambda_1} \cdots \frac{\exp(-\lambda_M z_M)}{\lambda_M} = \exp(-\lambda' z) \Big/ \prod_{m=1}^{M} (\lambda_m) \qquad (29)$$

if $\mathrm{Re}(\lambda_m) > 0$ for m=1:M. Therefore, average

$$a = e_z(z) = \frac{1}{(i2\pi)^M} \int_C d\lambda \; \mu_z(\lambda) \exp(-\lambda' z) \Big/ \prod_{m=1}^{M} (\lambda_m) \; , \qquad (30)$$

provided that the m-th Bromwich contour C_m stays to the <u>right</u> of the origin for m=1:M, and also stays within the ROA of joint MGF $\mu_z(\lambda)$. Relation (30) provides a method for obtaining the joint EDF $e_z(z)$ at arbitrary M-dimensional point z directly from the joint MGF $\mu_z(\lambda)$ without having to calculate or deal with joint PDF $p_z(z)$.

Example 4. $g_z(u_1,\ldots,u_M) = \delta(u_1-z_1)\ U(z_2-u_2)\ \cdots\ U(z_M-u_M)$. (31)

Average (14) is given by

$$a = \int_{-\infty}^{z_2} du_2 \cdots \int_{-\infty}^{z_M} du_M\ p_z(z_1,u_2,\ldots,u_M)\ , \tag{32}$$

which is 1 part PDF and M-1 parts CDF. M-dimensional field point $z = [z_1\ \cdots\ z_M]'$ is arbitrary. The gamma function (16), corresponding to nonlinearity (31), is

$$\gamma_z(\lambda) = \exp(-\lambda_1\ z_1) \int_{-\infty}^{z_2} du_2 \cdots \int_{-\infty}^{z_M} du_M\ \exp(-\lambda_2\ u_2 - \cdots -\lambda_M\ u_M) =$$

$$= \exp(-\lambda' z) \Big/ \prod_{m=2}^{M}(-\lambda_m) \quad \text{if } \mathrm{Re}(\lambda_m) < 0 \text{ for } m=2{:}M\ . \tag{33}$$

There is no restriction on λ_1 in this particular gamma function. The alternative form for average a in equation (32) is given by

$$a = \frac{1}{(i2\pi)^M} \int_C d\lambda\ \mu_z(\lambda)\ \exp(-\lambda' z) \Big/ \prod_{m=2}^{M}(-\lambda_m)\ , \tag{34}$$

provided that the m-th Bromwich contour C_m stays to the <u>left</u> of the origin for m=2:M, and also stays within the ROA of joint MGF $\mu_z(\lambda)$. The particular contour C_1 for m=1 can pass either to the right or left of the origin in the complex λ_1 plane but must stay within the ROA(μ_z).

Example 5. $$g_z(u_1,\ldots,u_M) = \prod_{m=1}^{M}\left(U(u_m-z_{ma}) - U(u_m-z_{mb})\right) , \qquad (35)$$

where $z_{ma} < z_{mb}$ for m=1:M. The difference of unit step functions is a unit pulse over interval (z_{ma},z_{mb}). Average (14) is now

$$a = \int_{z_{1a}}^{z_{1b}} du_1 \cdots \int_{z_{Ma}}^{z_{Mb}} du_M \; p_z(u_1,\ldots,u_M) = Pr(z_{1a}<z_1<z_{1b},\ldots,z_{Ma}<z_M<z_{Mb}) \qquad (36)$$

which is recognized as a set of joint interval probabilities. Limits $\{z_{ma}\}$ and $\{z_{mb}\}$ are arbitrary. The gamma function (16) corresponding to nonlinearity (35) is given by

$$\gamma_z(\lambda) = \prod_{m=1}^{M}\left\{\int_{z_{ma}}^{z_{mb}} du \; \exp(-\lambda_m u)\right\} = \prod_{m=1}^{M}\left\{\frac{\exp(-\lambda_m z_{ma}) - \exp(-\lambda_m z_{mb})}{\lambda_m}\right\} \qquad (37)$$

for <u>all</u> λ. The use of equation (37) in general relation (18) yields the alternative average form

$$a = \frac{1}{(i2\pi)^M}\int_C d\lambda \; \mu_z(\lambda) \prod_{m=1}^{M}\left\{\frac{\exp(-\lambda_m z_{ma}) - \exp(-\lambda_m z_{mb})}{\lambda_m}\right\} , \qquad (38)$$

where M-dimensional contour C is restricted only by being required to remain in the ROA of joint MGF $\mu_z(\lambda)$. These interval probabilities (38) can be determined directly from the joint MGF $\mu_z(\lambda)$ of RV z without the need to calculate or deal with the joint PDF $p_z(z)$ of RV z, as would be required by attempting to use equation (36).

Example 6. $g(u_1,\ldots,u_M) = u_1^{\nu_1-1} \cdots u_M^{\nu_M-1}$ for $u_m > 0$ (39)

and zero elsewhere; parameters $\nu_m > 0$ for m=1:M. Let $\{z_m\}$, m=1:M, be positive RVs with joint PDF p_z and joint MGF μ_z. The average (14) is given by

$$a = \int_0^\infty du_1 \cdots \int_0^\infty du_M \; u_1^{\nu_1-1} \cdots u_M^{\nu_M-1} \; p_z(u_1,\ldots,u_M) \;, \tag{40}$$

which is recognized as the (ν_m-1) th-order moments of RV z. The gamma function (16), corresponding to nonlinearity (39), is

$$\gamma(\lambda) = \prod_{m=1}^{M} \left\{ \int_0^\infty du_m \; u_m^{\nu_m-1} \; \exp(-\lambda_m \, u_m) \right\} = \prod_{m=1}^{M} \left\{ \frac{\Gamma(\nu_m)}{\lambda_m^{\nu_m}} \right\} \tag{41}$$

if $\mathrm{Re}(\lambda_m) > 0$ for m=1:M. The use of equation (41) in general relation (18) yields the alternative form

$$a = \prod_{m=1}^{M} \{\Gamma(\nu_m)\} \; \frac{1}{(i2\pi)^M} \int_{C_r} d\lambda \; \mu_z(\lambda) \Big/ \prod_{m=1}^{M} \left(\lambda_m^{\nu_m}\right) \;, \tag{42}$$

where C_r denotes that the M Bromwich contours $\{C_m\}$ must all pass to the right of the origin in their respective λ_m planes. There is no parameter vector z for this particular probabilistic problem (40).

Example 7. $g(u_1,u_2) = 1$ for $|u_1 \pm u_2| < 1$; zero otherwise. (43)

This two-dimensional nonlinearity is nonzero only within a unit diamond D centered at the origin. The average (14) is given by

$$a = \iint_D du_1\, du_2\, p_z(u_1,u_2) = Pr(z_1,z_2 \in D) \ , \tag{44}$$

which is the probability of RV $z = [z_1\ z_2]'$ landing in the unit diamond D located at the origin. The gamma function (16), corresponding to nonlinearity (43), is

$$\gamma(\lambda) = \iint_D du_1\, du_2\, \exp(-\lambda_1 u_1 - \lambda_2 u_2) =$$

$$= 4\, \frac{\cosh(\lambda_1) - \cosh(\lambda_2)}{\lambda_1^2 - \lambda_2^2} \quad \text{for } \underline{\text{all}}\ \lambda_1,\lambda_2 \ . \tag{45}$$

The use of equation (45) in general relation (18) leads to alternative form

$$a = \frac{4}{(i2\pi)^2} \int_C d\lambda\, \mu_z(\lambda)\, \frac{\cosh(\lambda_1) - \cosh(\lambda_2)}{\lambda_1^2 - \lambda_2^2} \ , \tag{46}$$

where contour C is restricted only to be in the ROA of joint MGF $\mu_z(\lambda)$.

Notice that nonlinearity $g(u_1,u_2)$ in equation (43) is not separable in the variables u_1,u_2; this is in contrast to the earlier six examples, where function $g(u_1,\ldots,u_M)$ was separable in all M variables $\{u_m\}$. Also, all the g-function examples here have been taken to be positive real where they are not zero.

SADDLEPOINT APPROXIMATION

The general M-dimensional integral of interest is given by equations (17) and (18) in the form

$$a = \frac{1}{(i2\pi)^M} \int_C d\lambda \; \mu_z(\lambda) \; \gamma(\lambda) = \frac{1}{(i2\pi)^M} \int_C d\lambda \; \exp[\Lambda(\lambda)] \; , \qquad (47)$$

where the function $\Lambda(\lambda)$ in equation (47) is defined as

$$\Lambda(\lambda) = \ln[\mu_z(\lambda) \; \gamma(\lambda)] = \chi_z(\lambda) + \ln \gamma(\lambda) \; , \qquad (48)$$

and where $\chi_z(\lambda)$ is the joint CGF (11) of RV z.

A real SP of the total integrand in equation (47) is located where the M partial derivatives (PDs) of $\exp[\Lambda(\lambda)]$ are all equal to zero. Equivalently, a real SP $\hat{\lambda}$ is located where the PDs

$$\left.\frac{\partial \Lambda(\lambda)}{\partial \lambda_m}\right|_{\hat{\lambda}} = 0 \quad \text{for m=1:M} \; . \qquad (49)$$

Saddlepoint equation (49) constitutes M nonlinear simultaneous equations in real variables $\{\lambda_m\}$, m=1:M. The location of the real SP $\hat{\lambda}$ depends on both $\chi_z(\lambda)$ and $\gamma(\lambda)$. Also, SP $\hat{\lambda}$ must lie in the intersection $\text{ROA}(\mu_z, \gamma)$ of their two ROAs. The M-dimensional contour C in equation (47) can be taken to pass through this real SP; that is, each Bromwich contour C_m passes through real component $\hat{\lambda}_m$ of real vector SP $\hat{\lambda}$. At this stage, there are no approximations involved in expression (47); this is an exact result for the average a of interest.

DERIVATION OF SADDLEPOINT APPROXIMATION

Once the real SP $\hat{\lambda}$ in the ROA(μ_z,γ) has been located, expand the $\Lambda(\lambda)$ function in equation (48) about that point according to M-dimensional Taylor series

$$\Lambda(\lambda) = \Lambda(\hat{\lambda}) + \sum_{m=1}^{M} \left.\frac{\partial \Lambda(\lambda)}{\partial \lambda_m}\right|_{\hat{\lambda}} \left(\lambda_m - \hat{\lambda}_m\right) +$$

$$+ \frac{1}{2} \sum_{m,\underline{m}=1}^{M} \Lambda_2(m,\underline{m}) \left(\lambda_m - \hat{\lambda}_m\right)\left(\lambda_{\underline{m}} - \hat{\lambda}_{\underline{m}}\right) + \cdots \qquad (50)$$

where $\hat{\lambda}_m$ is real and second-order coefficients

$$\Lambda_2(m,\underline{m}) \equiv \left.\frac{\partial^2 \Lambda(\lambda)}{\partial \lambda_m \, \partial \lambda_{\underline{m}}}\right|_{\hat{\lambda}} \quad \text{for } m,\underline{m}=1:M \ . \qquad (51)$$

Also, define the MxM Hessian matrix of $\Lambda(\lambda)$ at the SP $\hat{\lambda}$ as

$$\Lambda_2 \equiv [\Lambda_2(m,\underline{m})] \ , \quad m,\underline{m}=1:M \ . \qquad (52)$$

Now, truncate expansion (50) at second order, use equation (49), and substitute the result into equation (47) to get the approximation

$$a_0 \equiv \frac{1}{(i2\pi)^M} \int_C d\lambda \, \exp\left[\Lambda(\hat{\lambda}) + \frac{1}{2} \sum_{m,\underline{m}=1}^{M} \Lambda_2(m,\underline{m}) \left(\lambda_m - \hat{\lambda}_m\right)\left(\lambda_{\underline{m}} - \hat{\lambda}_{\underline{m}}\right)\right] \qquad (53)$$

At this point, make the change of variable

$$\lambda_m = \hat{\lambda}_m + i \, s_m \quad \text{for } m=1:M \ , \qquad (54)$$

and define Mx1 real vector $s = [s_1 \cdots s_M]'$. Then, equation (53)

yields

$$a_0 = \frac{\exp[\Lambda(\hat{\lambda})]}{(2\pi)^M} \int_{-\infty}^{\infty} ds \exp\left[-\frac{1}{2} \sum_{m,\underline{m}=1}^{M} \Lambda_2(m,\underline{m})\ s_m\ s_{\underline{m}}\right] =$$

$$= \frac{\exp[\Lambda(\hat{\lambda})]}{(2\pi)^{M/2} \left[\det(\Lambda_2)\right]^{\frac{1}{2}}} , \qquad (55)$$

where equation (52) has been used. This result, a_0, in equation (55) is denoted as the zeroth-order saddlepoint approximation to exact result a. Observe that a_0 must always be positive, since MxM Hessian matrix Λ_2 is always positive definite at real SP $\hat{\lambda}$ if g(u) in equation (18) is real and non-negative for all u.

CORRECTIONS TO SADDLEPOINT APPROXIMATION

The first-order correction to a_0 is given in reference 1, pages 15 - 16, as

$$a_1 \equiv a_0\ [1 + c_t] , \qquad (56)$$

where c_t is a correction term. Alternatively, the exponential version of the saddlepoint correction is (reference 3, page 180)

$$a_e \equiv a_0 \exp(c_t) , \qquad (57)$$

which has the same first-order term as equation (56). However, it has been found numerically that approximation a_e generally gives more accurate results than either a_0 or a_1; accordingly, a_e has been used for the majority of the numerical results to be presented here.

The correction term c_t uses the third- and fourth-order PDs of the function $\Lambda(\lambda)$, defined in equation (48); however, these particular PDs only need to be evaluated at the real saddlepoint $\hat{\lambda}$.

Expressions were given earlier for the gamma function $\gamma(\lambda)$ corresponding to the joint CDF, EDF, PDF, moments, and interval probabilities. Also, the joint MGF $\mu_z(\lambda)$ can be found in closed form for a number of statistics, such as the joint Gaussian, quadratic and linear forms in dependent Gaussian RVs, and linearly transformed independent RVs with arbitrary statistics. By combining these results with equations (55) - (57), SPAs can now be obtained for a number of M-dimensional probabilistic problems that were previously considered unsolvable. These SPAs require that the M-dimensional field point, z, of interest be specified and that the real SP $\hat{\lambda}$ in the ROA(μ_z,γ) be obtained.

Strictly speaking, closed forms for joint MGF $\mu_z(\lambda)$ or joint CGF $\chi_z(\lambda)$ are not mandatory; however, it must be possible to numerically evaluate $\mu_z(\lambda)$ or $\chi_z(\lambda)$ at any M-dimensional real point λ required. Then, a numerical search for the minimum of total integrand $\mu_z(\lambda)\ \gamma(\lambda)$ or $\chi_z(\lambda) + \ln \gamma(\lambda)$ of equations (47) and (48), where the search can be confined to the real $\{\lambda_m\}$ axes, will locate the real SP $\hat{\lambda}$ in the ROA. The Hessian matrix Λ_2 in equation (52) will then require second-order differences of $\Lambda(\lambda)$ be taken in the neighborhood of the SP $\hat{\lambda}$. Numerical evaluation of third- and fourth-order PDs may be questionable, however.

CUMULATIVE DISTRIBUTION FUNCTION OF THE MAXIMUM OF M DEPENDENT RANDOM VARIABLES

RV $\mathbf{z} = [z_1 \cdots z_M]'$ has statistically dependent components $\{z_m\}$, m=1:M. The maximum RV of set $\{z_m\}$ is defined as

$$\mathbf{y} = \max(z_1,\ldots,z_M) \ , \tag{58}$$

which is a random scalar. The first-order CDF of RV $\mathbf{y}$ is

$$c_{\mathbf{y}}(y) = \Pr(\mathbf{y} < y) = \Pr(z_1 < y,\ldots, z_M < y) = c_{\mathbf{z}}(y,\ldots,y) =$$

$$= \frac{1}{(i2\pi)^M} \int_{C_1} d\lambda \ \mu_{\mathbf{z}}(\lambda) \ \exp\Big(- y \sum_{m=1}^{M} \lambda_m\Big) \Big/ \prod_{m=1}^{M}(-\lambda_m) \ , \tag{59}$$

where M-dimensional contour C_1 denotes that the Bromwich contours must all pass to the left of their respective origins. Equation (59) is a single M-dimensional integral for the CDF of maximum RV $\mathbf{y}$ that allows for arbitrary statistical dependencies between RVs $\{z_m\}$, as reflected through the joint MGF $\mu_{\mathbf{z}}(\lambda)$.

The $\Lambda(\lambda)$ function of equation (48) is given here by

$$\Lambda(\lambda) = \chi_{\mathbf{z}}(\lambda) - y \sum_{m=1}^{M} \lambda_m - \sum_{m=1}^{M} \ln(-\lambda_m) \ . \tag{60}$$

The first-order PDs of $\Lambda(\lambda)$ are

$$\frac{\partial \Lambda(\lambda)}{\partial \lambda_m} = \frac{\partial \chi_{\mathbf{z}}(\lambda)}{\partial \lambda_m} - y - \frac{1}{\lambda_m} \quad \text{for m=1:M} \ . \tag{61}$$

The SP equations are obtained by setting these M PDs to zero and numerically solving for M-dimensional SP $\hat{\lambda}$. However, the search

for the real SP solution of equation (61) must be conducted only in the left half of each real λ_m axis and within the ROA of joint MGF $\mu_z(\lambda)$. The search procedure must not be allowed to wander into any of the right half real λ_m axes; otherwise, the search may drift off to infinity or find a spurious real point of the analytic continuation of $\mu_z(\lambda)$ outside the ROA(μ_z,γ) that also satisfies the SP equations.

The second-order PDs of $\Lambda(\lambda)$ follow from equation (61) as

$$\frac{\partial^2 \Lambda(\lambda)}{\partial \lambda_m \, \partial \lambda_{\underline{m}}} = \frac{\partial^2 \chi_z(\lambda)}{\partial \lambda_m \, \partial \lambda_{\underline{m}}} + \frac{1}{\lambda_m^2} \delta_{m\underline{m}} \quad \text{for } m,\underline{m}=1:M \; . \tag{62}$$

The addition of the positive diagonal terms $\{1/\lambda_m^2\}$ (at the real SP) to the Hessian matrix of $\chi_z(\lambda)$ serves only to improve the positive definiteness of the Hessian matrix (62) for $\Lambda(\lambda)$. Equations (60) through (62) enable calculation of the zeroth-order SPA a_0 given by equation (55). The correction term c_t in equations (56) and (57) also requires the third- and fourth-order PDs of $\Lambda(\lambda)$ and can be derived from equation (62).

TWO TEST EXAMPLES

Two test examples will be used extensively in the following developments. They are

1. Joint Gaussian RVs $\{z_m\}$, m=1:M, with arbitrary M×1 mean vector and M×M covariance matrix, and

2. Linearly transformed exponential RVs $\{e_n\}$, n=1:N. In particular, RV z = A e, where Nx1 RV e is composed of independent, identically distributed RVs, each with PDF exp(-u) for u > 0. Arbitrary matrix A is MxN, thereby making z an Mx1 RV with dependent non-Gaussian components $\{z_m\}$.

The following numerical examples all employ M = 4 and N = 7. Since there are no analytic results for the statistics of maximum variate y defined in equation (58), when components $\{z_m\}$ are statistically dependent, three different methods are employed to determine the "truth" for comparison with the SPAs that are developed here; they are Gauss-Hermite quadrature for the lower tail of RV y, simulation using 1e8 trials for the central region, and an asymptotic form for the upper tail of RV y.

To employ Gauss-Hermite quadrature on the exact M-dimensional integral (47), the contour C is first moved to the real SP of total integrand $\exp[\Lambda(\lambda)]$. Then, an M-dimensional linear transformation of variables is utilized that makes the form of the new integrand, in the neighborhood of the SP, behave as

$$\exp\left[-\frac{1}{2}\left(s_1^2 + \cdots + s_M^2\right)\right] , \tag{63}$$

where s_m is the vertical deviation from the real SP in the complex λ_m plane. Finally, the standard one-dimensional Gauss-Hermite relations are replicated in all M dimensions, using the weighting factor (63). The number of samples per dimension is

increased until stability in the estimated integral is realized, or until storage and execution time problems become untenable. It has been found for the current two test cases that this Gauss-Hermite procedure is accurate enough only on the lower tail of maximum RV **y**.

The asymptotic EDF of maximum RV **y** is given as the sum of the first-order EDFs of each of the individual RVs $\{z_m\}$ in equation (58). This asymptotic result becomes relatively more accurate as the upper tail of RV **y** is examined. The combination of the three approaches above is sufficient to enable determination of the relative accuracies of the SPAs over essentially the full range of arguments of the various statistics considered here.

GRAPHICAL RESULTS

Figure 1 displays results for the CDF of maximum RV **y** for the Gaussian test example (GTE) cited earlier. The black curve is the simulation result (SIM) using 1e8 trials, while the x points are the SPAs obtained from exponential version a_e in equation (57). Equations (59) through (62) were used for these computations. The red curve is the asymptotic result (ASY) for the CDF of **y**; the asymptotic result corroborates the simulation in the central region and significantly extends the CDF simulation on the upper tail. On the lower tail, the asymptotic result is useless.

Figure 2 contains plots (for the GTE) of the ratio of SPA a_e to the three attempts at "truth", to be called accuracy ratios. Gauss-Hermite quadrature is denoted by GHQ, the simulation by SIM, and asymptotic by ASY. The GHQ curve can be trusted for threshold argument y less than 1, the SIM curve for y larger than 0, and the ASY curve for y larger than 6. The end result is that the SPA a_e varies from +3% to -8% error over the complete range of its argument values. The notation NG denotes regions where the plotted results are no good and cannot be used.

Figure 3 displays results for the CDF of maximum RV y for the exponential test example (ETE) cited earlier. The superposed points labeled with O are the SPAs obtained from the zeroth-order SPA a_0 in equation (55). Approximation a_0 is significantly poorer than exponential SPA a_e; in fact, a_0 becomes larger than 1 for threshold argument y larger than 7; although SPA a_0 must be positive, it need not stay below 1. By contrast, SPA a_e stays below 1 for all y for these examples. An asymptotic result for the CDF of RV y was not computed for this ETE.

Figure 4 contains the accuracy ratios for the ETE. The zeroth-order approximation a_0 has error variations from -70% to +35%, whereas a_e only errs by -20% to +4%. This example illustrates the need to compute the correction term c_t for use in equation (57). Of course, the additional effort required to evaluate the third- and fourth-order PDs needed for c_t can be considerable; see reference 1 for an example.

NEED TO RESORT TO EDF OF MAXIMUM VARIATE y

For scalar RV y, the EDF is simply $e_y(y) = 1 - c_y(y)$, from which the detection probability P_d and false alarm probability P_f of a threshold-comparison processor can be immediately calculated according to $P_d = 1 - c_y(y|H_1)$ and $P_f = 1 - c_y(y|H_0)$, where H_1 and H_0 are the hypotheses that a signal is present and absent, respectively. If the CDF values $c_y(y)$ were exact, these relations could be used directly. However, small approximation errors in calculating the CDF values $c_y(y)$ can sometimes result in large EDF errors, depending on the exact range under consideration.

For example, if the exact P_d is 0.99, then $c_y(y|H_1) = 0.01$. However, the SPA to this CDF may be $0.01\ (1 + \varepsilon)$, where ε is in the range ± 0.1. This result leads to an SPA for P_d of value $1 - 0.01\ (1 + \varepsilon) = 0.99 - 0.01\ \varepsilon$ = (0.989 to 0.991). This range of variation is probably quite acceptable for P_d evaluation.

On the other hand, suppose the exact P_f is 0.001, meaning $c_y(y|H_0) = 0.999$. But, for c_y SPA $0.999\ (1 + \varepsilon)$, the SPA to P_f is $1 - 0.999\ (1 + \varepsilon) = 0.001 - 0.999\ \varepsilon$ = (-0.099 to 0.101). This range is totally unacceptable. Thus, it is necessary to have a method for <u>direct</u> calculation of the EDF $e_y(y)$ itself of maximum RV y, especially for very small EDF or P_f values.

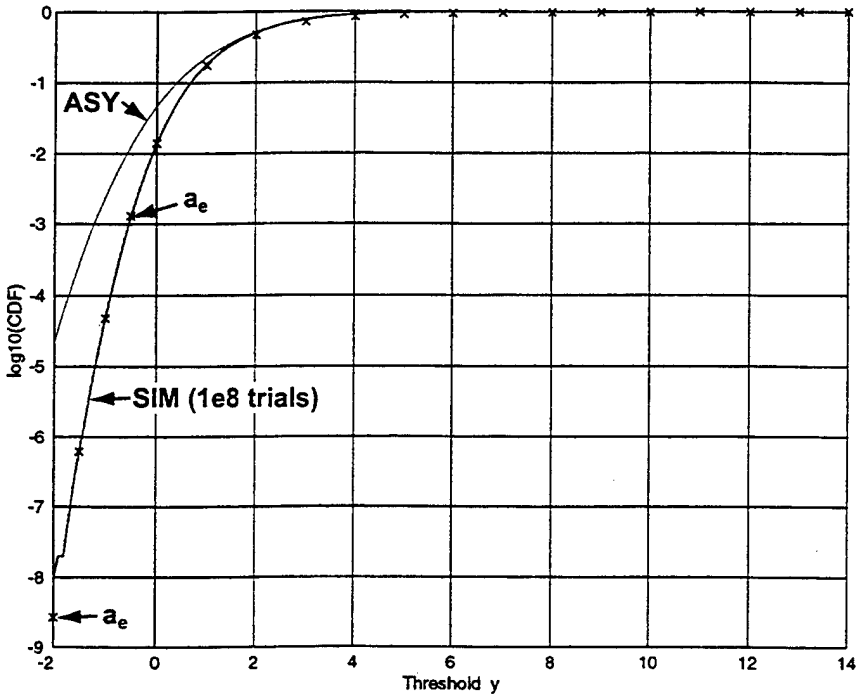

Figure 1. CDF of Maximum RV for GTE

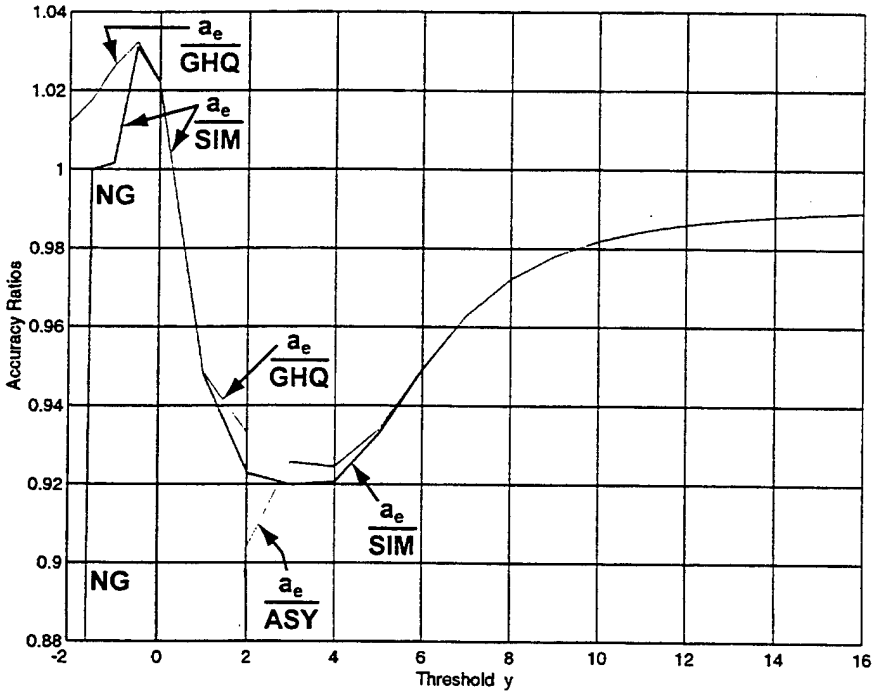

Figure 2. Accuracy Ratios for CDF of Maximum RV for GTE

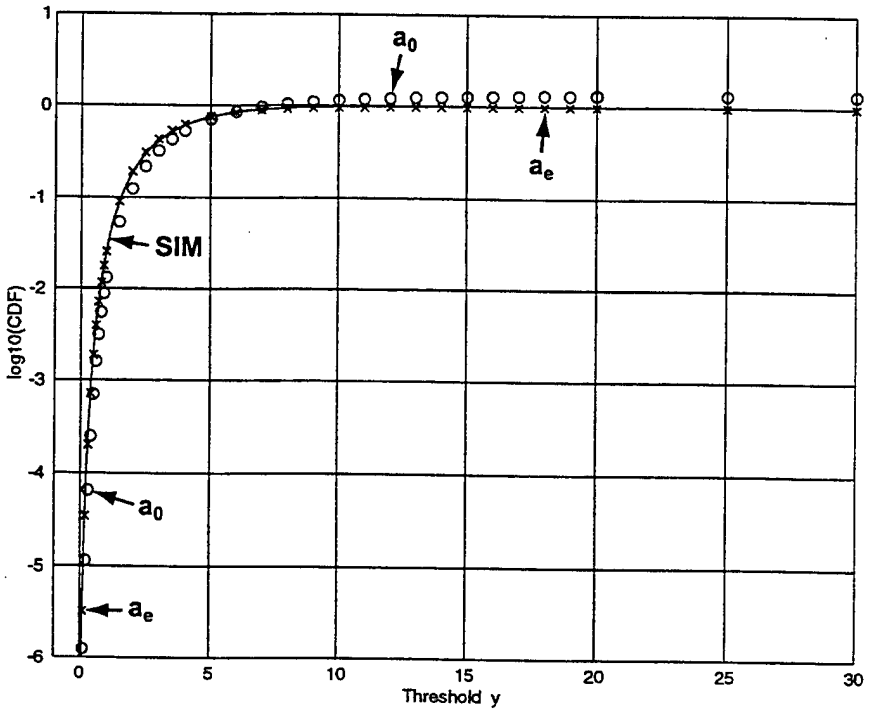

Figure 3. CDF of Maximum RV for ETE

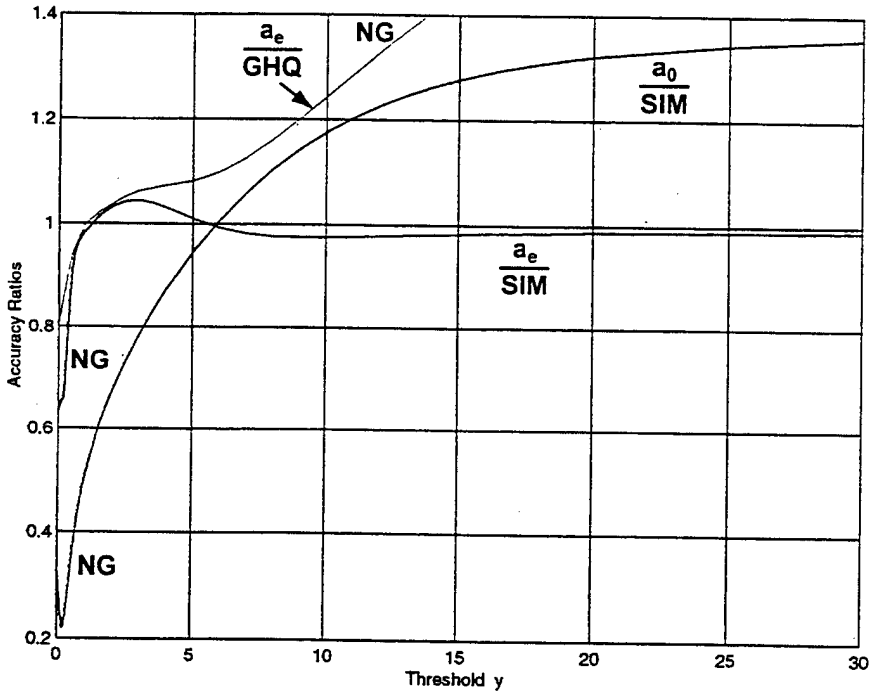

Figure 4. Accuracy Ratios for CDF of Maximum RV for ETE

EXCEEDANCE DISTRIBUTION FUNCTION OF THE MAXIMUM OF M DEPENDENT RANDOM VARIABLES

The first-order EDF of maximum variate y in equation (58) is not as simple as that given for the CDF in equation (59). The added complexity for the EDF is best illustrated by considering the special case of M = 2; that is, $y = \max(z) = \max(z_1, z_2)$.

EXCEEDANCE DISTRIBUTION FUNCTION OF y FOR M = 2

For M = 2, there follows $y = \max(z_1, z_2)$. Consider a two-dimensional z_1, z_2 plane with horizontal and vertical lines drawn at threshold y in both dimensions. Label the quadrants centered at the point (y,y) in the z_1, z_2 plane as Q_1, Q_2, Q_3, and Q_4, in standard order. Then, CDF $c_y(y) = \Pr(z_1 < y,\ z_2 < y) = c_z(y,y)$ is the probability of RV pair z_1, z_2 landing in quadrant Q_3.

On the other hand, EDF $e_y(y)$ is the probability of RV pair z_1, z_2 landing in quadrants Q_1, Q_2, or Q_4; call these individual quadrant probabilities P_1, P_2, and P_4, respectively. Thus, there follows, for the composite probability,

$$e_y(y) = P_1 + P_2 + P_4 =$$

$$= (P_1 + P_2) + (P_1 + P_4) - P_1 =$$

$$= (P_1 + P_4) + P_2 \ . \qquad (64)$$

The first form in equation (64) adds up positive numbers; however, there are three probability terms that have to be computed. The second form in equation (64) (called inclusion and exclusion) also requires that three different probabilities be calculated; additionally, it requires the subtraction of a positive quantity. Finally, the third form in equation (64) requires that only two terms be evaluated, both of which are positive. The third form in equation (64) can be interpreted as follows: $P_1 + P_4 = Pr(z_1 > y)$ and $P_2 = Pr(z_1 < y, z_2 > y)$. The P_2 term is a mixed probability, namely, 1 part CDF and 1 part EDF.

If the quadrant probabilities $\{P_k\}$, k=1:4, are not calculated exactly, but perhaps obtained by SPAs, the second form in equation (64) will be subject to possible loss of significance due to the negative term. Therefore, this second form is not recommended for use when only approximations to the individual probabilities are available. Also, forms 1 and 2 in equation (64) require three probability evaluations, whereas form 3 requires only two probability evaluations; this will become significant in M dimensions for M > 2.

EXCEEDANCE DISTRIBUTION FUNCTION OF y FOR M > 2

For general M, the maximum variate is given by equation (58) as $y = \max(z_1,\ldots,z_M)$. The EDF of RV y can be written as an obvious generalization of the third form of equation (64):

$$e_y(y) = \Pr(y > y) = \Pr(z_1 > y) + \Pr(z_1 < y,\ z_2 > y) +$$
$$+ \Pr(z_1 < y,\ z_2 < y,\ z_3 > y) + \cdots$$
$$+ \Pr(z_1 < y,\ldots,\ z_{M-1} < y,\ z_M > y)\ . \qquad (65)$$

Equation (65) contains M terms, all of which are positive; there are no cancellations involved in this form. Whereas the number of terms in form (65) increases only linearly with dimensionality M, by contrast the corresponding generalizations of forms 1 and 2 in equation (64) would involve $2^M - 1$ terms. Thus, the effort here will employ form (65) for all future calculations.

By reference to equations (5), (8), and (30), the EDF in equation (65) can be written as the sum of a number of contour integrals:

$$e_y(y) = \frac{1}{i2\pi}\int_{C_r} d\lambda_1\ \frac{\mu_1(\lambda_1)\ \exp(-y\lambda_1)}{\lambda_1} +$$

$$+ \frac{1}{(i2\pi)^2}\int_{C_l} d\lambda_1 \int_{C_r} d\lambda_2\ \frac{\mu_2(\lambda_1,\lambda_2)\ \exp(-y\lambda_1 - y\lambda_2)}{(-\lambda_1)(\lambda_2)} + \cdots \qquad (66)$$

$$+ \frac{1}{(i2\pi)^M}\int_{C_l} d\lambda_1 \cdots \int_{C_l} d\lambda_{M-1} \int_{C_r} d\lambda_M\ \frac{\mu_M(\lambda_1,\ldots,\lambda_M)}{(-\lambda_1)\cdots(-\lambda_{M-1})(\lambda_M)}\ \exp\left(-y\sum_{m=1}^{M}\lambda_m\right)$$

where auxiliary MGFs are defined at stage n as

$$\mu_n(\lambda_1,\ldots,\lambda_n) = \mu_z(\lambda_1,\ldots,\lambda_n,0,0,\ldots,0) \quad \text{for n=1:M} . \qquad (67)$$

Stage variable n varies from 1 to M. There immediately follows, from equation (67), the analogous auxiliary CGFs:

$$\chi_n(\lambda_1,\ldots,\lambda_n) = \chi_z(\lambda_1,\ldots,\lambda_n,0,0,\ldots,0) \quad \text{for n=1:M} . \qquad (68)$$

The result in equation (66) is exact. In order to calculate the EDF $e_y(y)$ via this equation, it is necessary to conduct one one-dimensional integral plus one two-dimensional integral plus ... plus one M-dimensional integral. To achieve the SPAs, this will entail determination of a one-dimensional real SP plus a two-dimensional real SP plus ... plus an M-dimensional real SP. Alternatively, the first few integrals in equation (66) could be conducted rather accurately via FFTs, if desired.

Since all the probabilities in equation (66) are positive, the corresponding SPAs are also positive. When a number of positive approximations are added, the general effect is to average the errors of each, and to realize some improvement of the accuracy. An exception occurs when one of the approximations has a very large error, in which case it may dominate the overall error of the sum. The least accurate SPAs to the individual terms in equation (66) are not known. The approach utilized here was to evaluate the SPAs for all the terms in equation (66) and add them; no FFTs were employed.

At the n-th stage of equation (66), the $\Lambda(\lambda)$ function of equation (48) takes the form

$$\Lambda_n(\lambda_1,\ldots,\lambda_n) = \chi_n(\lambda_1,\ldots,\lambda_n) - y\sum_{m=1}^{n}\lambda_m - \sum_{m=1}^{n-1}\ln(-\lambda_m) - \ln(\lambda_n) \ . \tag{69}$$

The PDs are given by

$$\frac{\partial\Lambda_n(\lambda_1,\ldots,\lambda_n)}{\partial\lambda_m} = \frac{\partial\chi_n(\lambda_1,\ldots,\lambda_n)}{\partial\lambda_m} - y - \frac{1}{\lambda_m} \quad \text{for } m=1:n \ . \tag{70}$$

Therefore, the nx1 SP vector $\hat{\lambda}^{(n)} = [\hat{\lambda}_1^{(n)}\cdots\ \hat{\lambda}_n^{(n)}]'$ at the n-th stage is the solution of the n simultaneous nonlinear equations

$$\left.\frac{\partial\chi_n(\lambda_1,\ldots,\lambda_n)}{\partial\lambda_m}\right|_{\hat{\lambda}^{(n)}} - y - \frac{1}{\hat{\lambda}_m^{(n)}} = 0 \quad \text{for } m=1:n \ . \tag{71}$$

Since the last contour in each integral in equation (66) must pass to the right of the origin in the complex λ_n plane, the n-th solution component, $\hat{\lambda}_n^{(n)}$ in equation (71), must be positive real. Conversely, all the other n-1 components of the SP vector $\hat{\lambda}^{(n)}$ must be negative real.

In order to effect the calculation of equation (66) for the total EDF $e_y(y)$, it is necessary to solve equation (71) repeatedly, as stage number n varies from 1 to M. Thus, the dimensionality of the SP search varies from n = 1 dimension to n = M dimensions. Then, all M SPAs to all the terms in equation (66) are added to yield the final approximation to the EDF $e_y(y)$.

GRAPHICAL RESULTS

Figure 5 displays the EDF $e_y(y)$ of maximum RV y for the GTE, as determined from equation (66). The curves have the same identifications as the CDF curves did earlier. The results for the asymptotic behavior and the SPA a_e overlie each other well into the upper tail, while the simulation estimates eventually become unstable due to an insufficient number of trials (1e8).

Figure 6 gives the corresponding accuracy ratios for this GTE. The SPA is off by -3% on the lower tail; this error increases to +1% for threshold y near 1; then, the error drifts down to almost -3% before turning up for large y arguments. There is an imprecise transition region for y in the range (8,13) where the simulation results are gradually replaced by the asymptotic results. The NG regions indicate where the curves should definitely be ignored. Again, Gauss-Hermite quadrature, simulation, and asymptotic behavior were employed to cover the entire range of argument values. The small errors for this GTE, namely ±3%, are very encouraging; this may be partially due to the averaging effects of the individual SPAs mentioned above.

Figure 7 displays the EDF results for the ETE. The SPA a_e and the asymptotic results overlie each other well into the upper tail. The accuracy ratios in figure 8 vary from -8% near y = 0, to +6% for y near 3. The simulation results in figures 7 and 8 for larger y, that is, the upper tail, cannot be trusted, due to instability. No asymptotic results were obtained for this ETE.

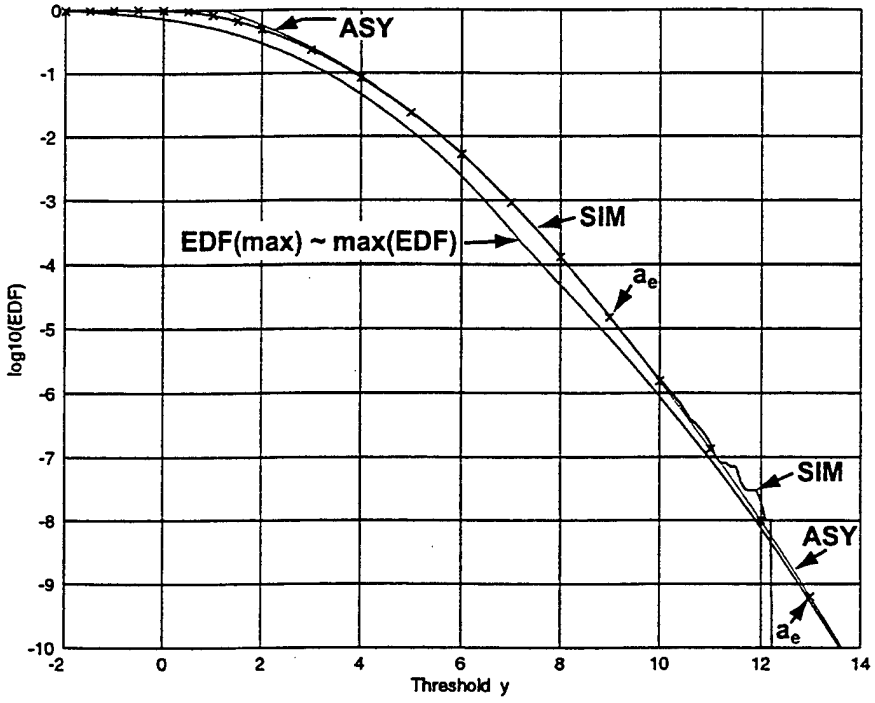

Figure 5. EDF of Maximum RV for GTE

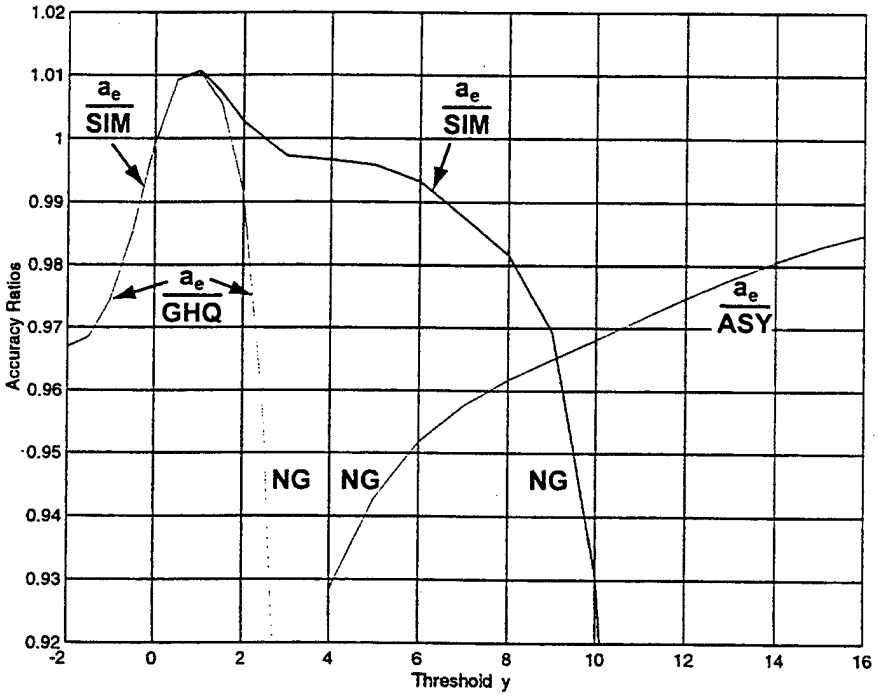

Figure 6. Accuracy Ratios for EDF of Maximum RV for GTE

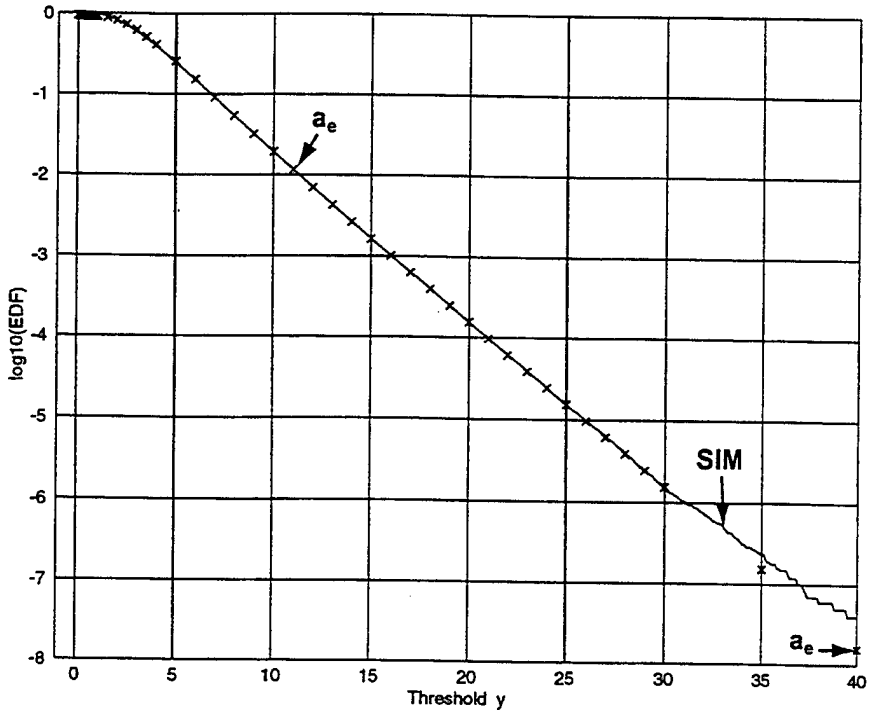

Figure 7. EDF of Maximum RV for ETE

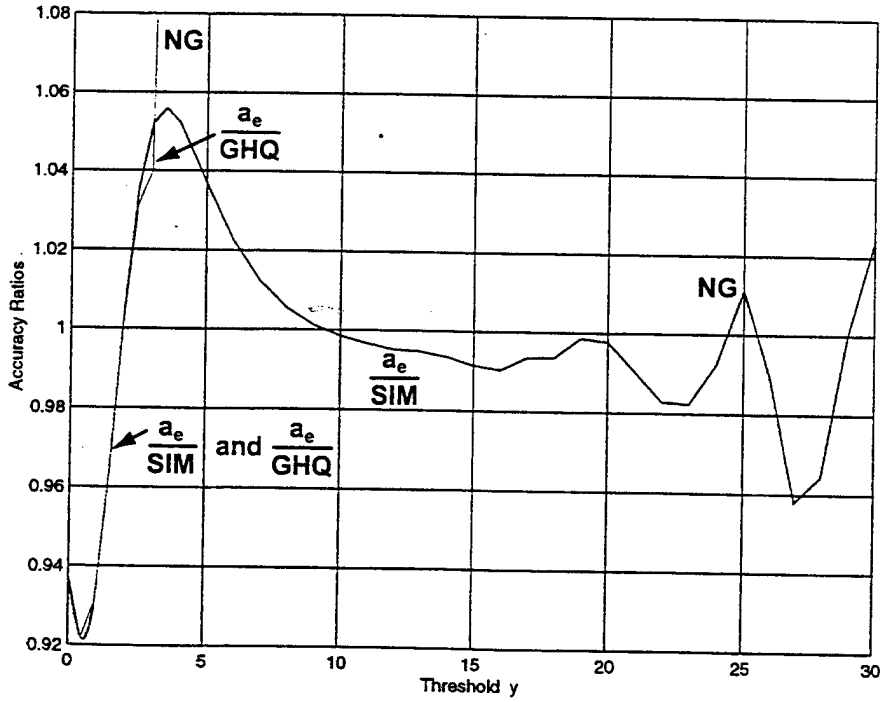

Figure 8. Accuracy Ratios for EDF of Maximum RV for ETE

PROBABILITY DENSITY FUNCTION OF THE MAXIMUM OF M DEPENDENT RANDOM VARIABLES

The interest in this section is on the first-order PDF of the maximum variate $y = \max(z_1,\ldots,z_M)$. One obvious possibility is to take the derivative of the first-order CDF $c_y(y)$ in equation (59) with respect to y. The result is

$$p_y(y) = \frac{1}{(i2\pi)^M} \int_{C_1} d\lambda\ \mu_z(\lambda)\ \exp\left(-y \sum_{m=1}^{M} \lambda_m\right) \sum_{m=1}^{M}(-\lambda_m) \Big/ \prod_{m=1}^{M}(-\lambda_m), \quad (72)$$

where the contours C_1 must pass to the left of the origins in each complex λ_m plane.

Direct use of equation (72) yielded a rather poor SPA to the PDF of y. This is believed to be due to the factor involving the sum of $(-\lambda_m)$ terms in the numerator of the integrand of equation (72). The joint MGF $\mu_z(\lambda)$, defined in equation (9), can be seen to decay in magnitude as λ deviates from the M-dimensional real SP $\hat{\lambda}$ on a Bromwich contour; the SP is located on the real axes of the complex planes $\{\lambda_m\}$, essentially because PDF p_z is a positive real function where it is nonzero. Likewise, the product in the denominator of equation (72) increases in magnitude as λ deviates from the real SP. Meanwhile, the exp factor in equation (72) maintains constant magnitude as λ deviates from the real SP along a Bromwich contour. The effect of the combination of these three factors alone would be to cause the magnitude of the integrand of equation (72) to decrease as λ deviates from the real SP; this is a favorable situation in which to develop an SPA.

However, the sum of the $(-\lambda_m)$ terms in the numerator of equation (72) increases as λ deviates from the real SP along a Bromwich contour. This increase in magnitude counters the desired decay of the total integrand in equation (72), which is required in order to achieve a reasonably accurate SPA. A numerical example employing equation (72) will be displayed shortly.

An approach that eliminates the troublesome summation factor from the numerator of equation (72) is to cancel each of the M terms, $-\lambda_m$, with the corresponding term in the denominator product. The net result can then be written as

$$p_y(y) = \sum_{n=1}^{M} \frac{1}{(i2\pi)^M} \int_{C^{(n)}} d\lambda \; \mu_z(\lambda) \exp\left(-y \sum_{m=1}^{M} \lambda_m\right) \Big/ \prod_{\substack{m=1 \\ m\neq n}}^{M} (-\lambda_m) \quad , \quad (73)$$

where all the integrals at the n-th stage are M-dimensional. Also, the M-dimensional contour $C^{(n)}$ changes with stage number n. Component contours $C_m^{(n)}$ pass to the left of the origin for m=1:M, $m\neq n$, while contour $C_n^{(n)}$ is arbitrary. Of course, $C^{(n)}$ must also stay within the ROA(μ_z) for each n=1:M.

The major difficulty with equation (73) is that it requires M M-dimensional integrals, whereas equation (72) only required one M-dimensional integral. Thus, it will be necessary to locate M M-dimensional real SPs for equation (73). Also, the question arises as to whether all the terms in equation (73) are positive.

DIRECT PROBABILITY DENSITY FUNCTION DETERMINATION

A direct determination of the PDF of maximum RV **y**, which is guaranteed to have all positive terms, will now be derived. Consider threshold value y and an infinitesimal increment dy located at y. Then, if $p_{\mathbf{y}}(y)$ is the PDF of maximum RV **y**, the quantity $p_{\mathbf{y}}(y)\,dy$ can be interpreted as the probability that the largest RV **y** lies in the interval (y,y+dy). But, there are M ways that this event can occur: RV z_m could lie in this interval while all M-1 of the other RVs $\{z_m\}$ lie below threshold y. Since m can vary from 1 to M, it is necessary to sum over the probabilities of each event, getting total

$$\begin{aligned} p_{\mathbf{y}}(y)\,dy &= \Pr(y < \mathbf{y} < y+dy) = \\ &= \Pr(y < z_1 < y+dy,\ z_2 < y, \ldots,\ z_M < y) + \cdots \\ &+ \Pr(z_1 < y, \ldots,\ z_{M-1} < y,\ y < z_M < y+dy)\ . \end{aligned} \tag{74}$$

All M terms in equation (74) are certainly positive, being probabilities. The probabilities of events involving more than one hit in the interval of width dy are of order dy^2 or higher, and are therefore negligible.

To illustrate the transformation of equation (74) into the λ domain, consider the first term and define nonlinear function

$$g_1(u_1,\ldots,u_M) = [U(u_1-y) - U(u_1-y-dy)]\ U(y-u_2) \cdots U(y-u_M)\ . \tag{75}$$

Then, the average

$$a_1 = \int du\ p_z(u)\ g_1(u) = \int_y^{y+dy} du_1 \int_{-\infty}^{y} du_2 \cdots \int_{-\infty}^{y} du_M\ p_z(u_1,\ldots u_M) \quad (76)$$

is immediately recognized as the first term on the right-hand side of equation (74). The gamma function corresponding to nonlinear function g_1 in equation (75) is

$$\gamma_1(\lambda) = \int_y^{y+dy} du_1 \int_{-\infty}^{y} du_2 \cdots \int_{-\infty}^{y} du_M\ \exp(-\lambda' u) =$$

$$= dy\ \exp\left(y \sum_{m=1}^{M}(-\lambda_m)\right) \Big/ \prod_{m=2}^{M}(-\lambda_m) \quad (77)$$

if $\mathrm{Re}(\lambda_m) < 0$ for m=2:M. Substitution of equation (77) into equation (18) yields the alternative

$$a_1 = \frac{dy}{(i2\pi)^M} \int_{C^{(1)}} d\lambda\ \mu_z(\lambda)\ \exp\left(y \sum_{m=1}^{M}(-\lambda_m)\right) \Big/ \prod_{m=2}^{M}(-\lambda_m)\ , \quad (78)$$

provided that contour $C_m^{(1)}$ passes to the left for m=2:M, while contour $C_1^{(1)}$ is arbitrary, but within the $\mathrm{ROA}(\mu_z)$.

Continuing this procedure for the remaining terms in equation (74) leads to the result $p_y(y)\ dy = a_1 + \cdots + a_M$, at which point the cancellation of common factor dy leads precisely to equation (73). Thus, it can be concluded that all M integrals in equation (73) will yield positive values and, therefore, positive SPAs. Equation (73) will require a solution for M M-dimensional real SPs and an evaluation of M M-dimensional integrals for the SPAs.

SADDLEPOINT EQUATIONS

At the n-th stage, n=1:M, the $\Lambda(\lambda)$ function of equation (48) takes the form, from equation (73),

$$\Lambda_n(\lambda) = \chi_z(\lambda) - y \sum_{m=1}^{M} \lambda_m - \sum_{\substack{m=1 \\ m\neq n}}^{M} \ln(-\lambda_m) \ . \tag{79}$$

The PDs are then

$$\frac{\partial \Lambda_n(\lambda)}{\partial \lambda_m} = \frac{\partial \chi_z(\lambda)}{\partial \lambda_m} - y - \frac{1}{\lambda_m} + \frac{1}{\lambda_n} \delta_{mn} \quad \text{for } m=1:M \ , \tag{80}$$

leading to the SP equations at the n-th stage,

$$\left.\frac{\partial \chi_z(\lambda)}{\partial \lambda_m}\right|_{\hat{\lambda}(n)} - y - \frac{1}{\hat{\lambda}_m^{(n)}} + \frac{1}{\hat{\lambda}_n^{(n)}} \delta_{mn} = 0 \quad \text{for } m=1:M \ . \tag{81}$$

The M-dimensional real SP vector $\hat{\lambda}^{(n)}$ must have $\hat{\lambda}_m^{(n)} < 0$ for m=1:M, $m\neq n$; however, component $\hat{\lambda}_n^{(n)}$ is arbitrary, but within the ROA(μ_z). Also, the solution of equation (81) must be conducted repeatedly for stage number n=1:M. Thus, M M-dimensional SPs must be computed and M M-dimensional SPAs obtained; when added together, they will constitute the total SPA to the PDF of maximum RV y.

GRAPHICAL RESULTS

Figure 9 presents the simulation and SPA results for the PDF of maximum RV **y** for the GTE, in addition to the asymptotic behavior. Whereas the simulation results become unstable for threshold y greater than 10, the SPA a_e and asymptotic curves continue to track each other well down on the upper tail. On the lower tail, the SPA tracks the rapid drop-off of the PDF while the simulation becomes untrustworthy.

Figure 10 is a repeat of figure 9 except that the scales have been changed and the SPA of the single integral approach in equation (72) has been added, as labeled with symbol O. Although this latter SPA is excellent on the lower tail, it deviates significantly on the upper tail, yielding useless results in that region. A possible reason for this behavior was discussed in the sequel to equation (72).

Figure 11 gives the accuracy ratios for this GTE. By piecing together the GHQ, SIM, and ASY results, it is estimated that the SPA for the PDF of RV **y** is about ±5% in error over the complete range of threshold y. There is an additional curve labeled a_e/dPDF, which is an attempt at approximating the PDF by using local differences of the corresponding CDF. Although adequate on the lower tail, the dPDF approximation quickly becomes unusable for moderate y values; the explanation for this degradation will be presented shortly.

Figure 12 displays the PDF results for the ETE. Again, the SPA a_e has no trouble tracking the PDF on both tails as well as the central region. The simulation results utilized a bin width of 0.1, thereby realizing relatively few hits per bin on the upper tail, at least for the 1e8 trials used. The SPA a_e can be seen tracking right through the middle of a smoothed version of the simulation PDF estimate.

Figure 13 contains the accuracy ratios for this ETE. On the lower tail, the SPA is in error by -30%, while in the central region, the relative error is about ±5%. The simulation estimates on the upper tail cannot be trusted; no asymptotic results were derived for this example.

DANGER OF USING DIFFERENCES OF CDF SPA VALUES

Due to the large amount of effort required to evaluate the PDF $p_y(y)$ of RV y by means of equation (73), an attempt was made to estimate the PDF by taking local differences of the CDF $c_y(y)$ in equation (59); the latter formula only requires one M-dimensional integral instead of M M-dimensional integrals. To ascertain the limitations of this approach, consider the PDF approximation at argument x obtained by the ratio

$$\frac{c(x + \Delta) - c(x - \Delta)}{2\Delta} \equiv p_a(x) \ . \qquad (82)$$

If CDF c is exact, the error in approximation (82) is of the order of Δ^2; that is, $p_a(x) = p(x) + O(\Delta^2)$, where p(x) is the exact value of the PDF at x.

However, if the CDF values are themselves approximations, the estimated PDF takes the form

$$\frac{(1 + \varepsilon_1)\, c(x + \Delta) - (1 + \varepsilon_2)\, c(x - \Delta)}{2\Delta} \equiv p_b(x) \ . \qquad (83)$$

This can be expanded as

$$p_b(x) = p_a(x) + \frac{\varepsilon_1 - \varepsilon_2}{2\Delta}\, c(x) + \frac{\varepsilon_1 + \varepsilon_2}{2}\, p(x) + O(\varepsilon\Delta) \ . \qquad (84)$$

Several possibilities exist. If $\varepsilon_1 = \varepsilon_2 = 0$, then $p_b(x) = p_a(x)$ given in equation (82). On the other hand, if $\varepsilon_1 = \varepsilon_2 = \varepsilon \neq 0$, then

$$p_b(x) = p_a(x) + \varepsilon\, p(x) \cong p(x)\, (1 + \varepsilon) \ , \qquad (85)$$

which is acceptable. However, if $\varepsilon_1 \neq \varepsilon_2 \neq 0$, and CDF value c(x) is not small, then the term $(\varepsilon_1 - \varepsilon_2)\, c(x)/(2\Delta)$ in equation (84) can be large relative to p(x); observe the division by the small quantity Δ. In fact, on the upper tail of an RV, the CDF c(x) is approaching 1 while the PDF p(x) is approaching zero, making the situation progressively worse. Thus, the use of equation (83) for approximating the PDF will certainly develop problems on the upper tail, and may develop problems earlier. Figure 11 is an illustration of this effect.

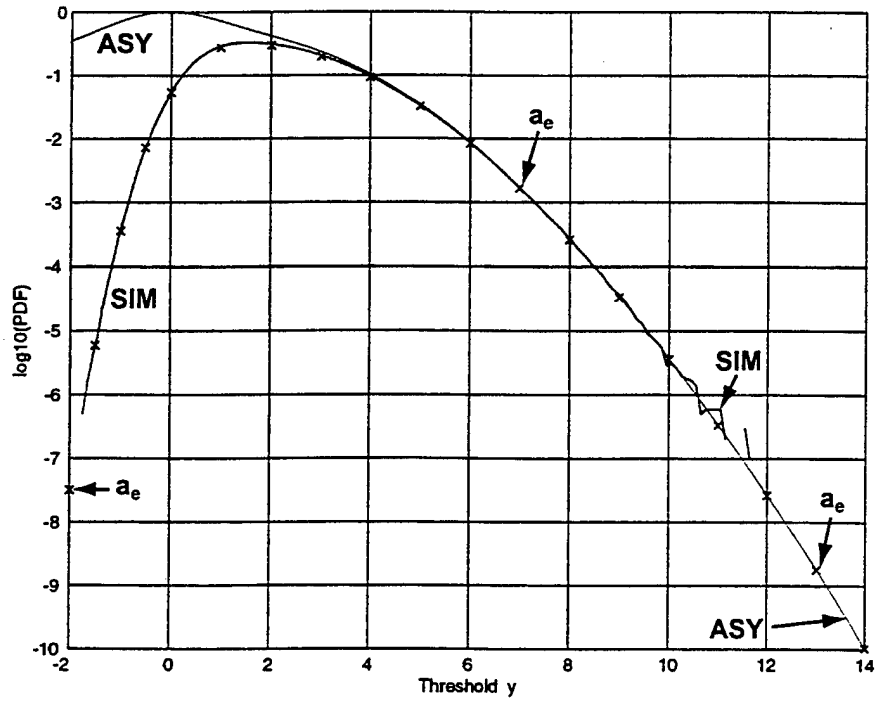

Figure 9. PDF of Maximum RV for GTE

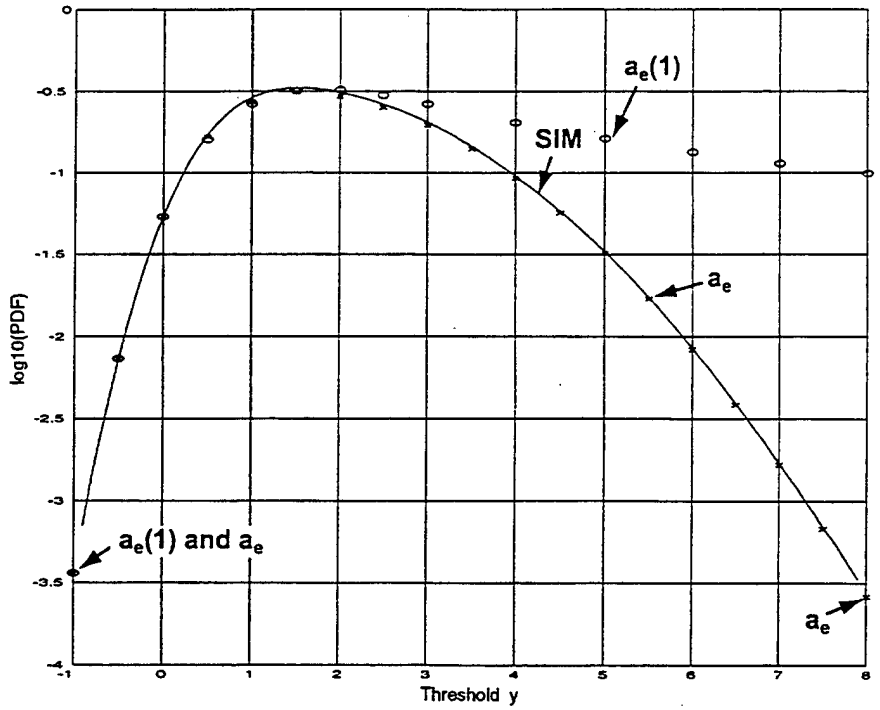

Figure 10. Shortcut PDF of Maximum RV for GTE

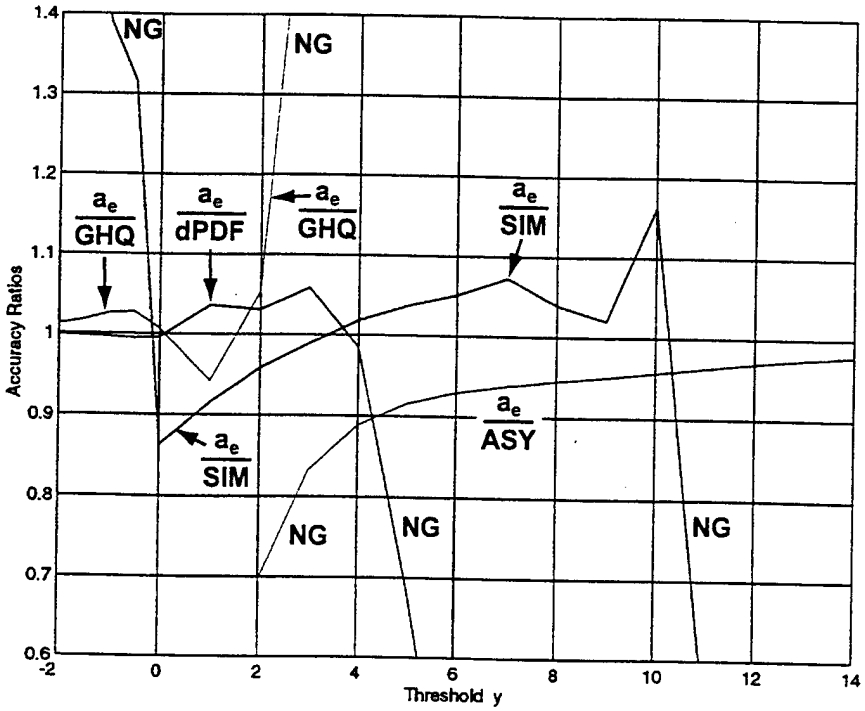

Figure 11. Accuracy Ratios for PDF of Maximum RV for GTE

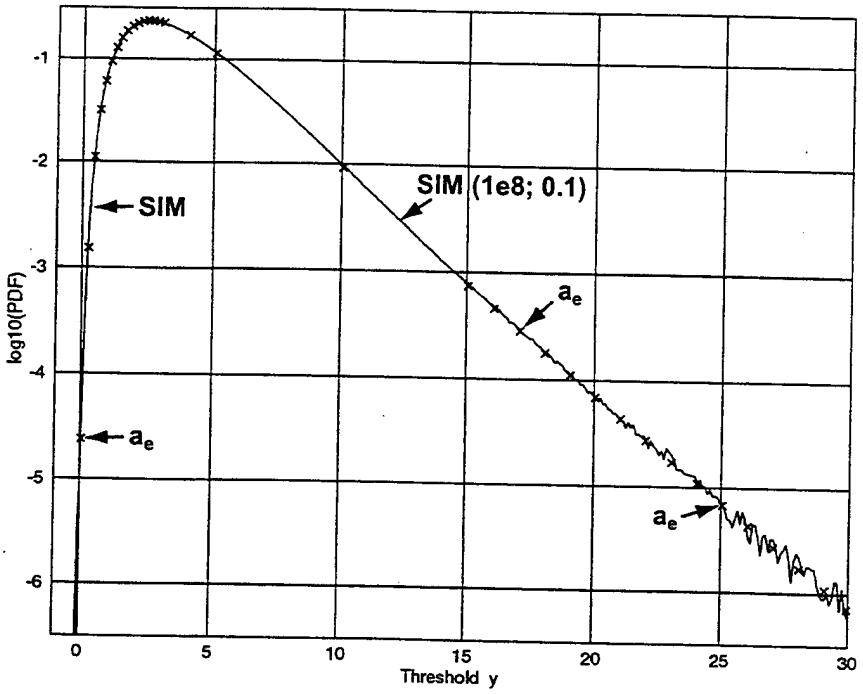

Figure 12. PDF of Maximum RV for ETE

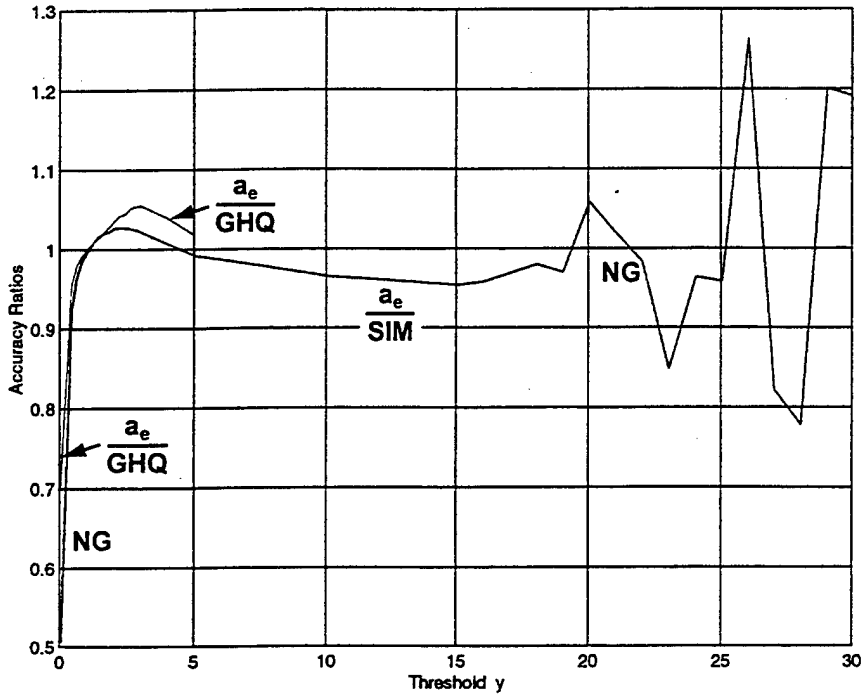

Figure 13. Accuracy Ratios for PDF of Maximum RV for ETE

STATISTICS OF THE RANGE VARIATE

Suppose RV $\mathbf{x} = [x_1 \cdots x_N]'$ is a set of N dependent RVs with joint MGF $\mu_{\mathbf{x}}(\alpha_1,\ldots,\alpha_N)$. The range variate for this set of N RVs is defined as

$$\mathbf{y} = \max(x_1,\ldots,x_N) - \min(x_1,\ldots,x_N) \ . \tag{86}$$

The first-order CDF, EDF, and PDF of random scalar $\mathbf{y}$ are of interest.

MATHEMATICAL MANIPULATIONS

In order to illustrate the procedure to be employed, a numerical example is used; namely, N is taken as 4, in which case equation (86) becomes

$$\mathbf{y} = \max(x_1,\ldots,x_4) - \min(x_1,\ldots,x_4) \ . \tag{87}$$

Equation (87) can be manipulated into a familiar form by defining the M = 12 (= N(N-1)) difference variables

$$\begin{aligned}
z_1 &= x_1 - x_2 \ , \quad & z_4 &= x_2 - x_1 \ , \quad & z_7 &= x_3 - x_1 \ , \quad & z_{10} &= x_4 - x_1 \ , \\
z_2 &= x_1 - x_3 \ , \quad & z_5 &= x_2 - x_3 \ , \quad & z_8 &= x_3 - x_2 \ , \quad & z_{11} &= x_4 - x_2 \ , \\
z_3 &= x_1 - x_4 \ , \quad & z_6 &= x_2 - x_4 \ , \quad & z_9 &= x_3 - x_4 \ , \quad & z_{12} &= x_4 - x_3 \ .
\end{aligned} \tag{88}$$

There follows, from equations (87) and (88),

$$\mathbf{y} = \max(z_1,\ldots,z_M) \ , \quad M = 12 \ , \tag{89}$$

while linear transformation (88) can be expressed as

$$\mathbf{z} = \mathbf{A}\,\mathbf{x} \ . \tag{90}$$

Matrix A is 12×4 (M×N) and has rank(A) = 3 (N-1). This can be deduced from equation (88) by noting that only three of the 12 RVs $\{z_m\}$ can be independently specified; the remainder follow as simple differences. (The remaining unlisted four differences that are possible in equation (87) are all zero and can never be the range variate.) Therefore, the joint PDF of RV z would involve a conditional component with 9 ($(N-1)^2$) delta functions. Nevertheless, SPAs can still be developed for the statistics of the range variate y, as given by equations (89) and (90).

Form (89) was encountered earlier in equation (58). The CDF of this form of RV y was given in equation (59), along with the $\Lambda(\lambda)$ function and its low-order PDs in equations (60) through (62). For easy reference, this last equation is repeated here:

$$\frac{\partial^2 \Lambda(\lambda)}{\partial \lambda_m \, \partial \lambda_{\underline{m}}} = \frac{\partial^2 \chi_z(\lambda)}{\partial \lambda_m \, \partial \lambda_{\underline{m}}} + \frac{1}{\lambda_m^2}\,\delta_{m\underline{m}} \quad \text{for } m,\underline{m}=1{:}M \ . \tag{91}$$

Although the M×M matrix of second-order PDs of $\chi_z(\lambda)$ has rank 3 (N-1), with three positive eigenvalues, the matrix of second-order PDs of $\Lambda(\lambda)$ has the full rank 12 (M) due to the $\{1/\lambda_m^2\}$ diagonal terms, and the Hessian matrix Λ_2 is positive definite. Thus, the determinant encountered in SPA a_0 in equation (55) is positive, and the SPA is well behaved.

The joint MGF $\mu_{\mathbf{z}}(\lambda)$ required for equation (91) can be obtained upon use of equation (90), according to expectation

$$\mu_{\mathbf{z}}(\lambda) = E \exp(\mathbf{z}'\lambda) = E \exp(\mathbf{x}'A'\lambda) = \mu_{\mathbf{x}}(A'\lambda) \ . \qquad (92)$$

The corresponding joint CGF is $\chi_{\mathbf{z}}(\lambda) = \chi_{\mathbf{x}}(A'\lambda)$. The vector λ is Mx1 while vector $A'\lambda$ is Nx1, which is the dimensionality of input RV $\mathbf{x}$ in equation (86).

A major drawback with form (89) for the range variate $\mathbf{y}$ is that the original set of N RVs in equation (86) has blossomed to the larger number of RVs, M = N(N-1). Therefore, the SP equations (61) now number M instead of N, making this a very difficult numerical problem for large M. For example, if N = 10, then M = 90, which means that a search in 90-dimensional λ-space is required. An attempt at reducing the number of RVs below the number M = N(N-1) required by formulation (88) was attempted by taking absolute values of the differences. Although this reduced the number of RVs $\{z_m\}$ to N(N-1)/2, the resulting SPA to the CDF of RV $\mathbf{y}$ was poorer than the approach using equation (88); the reason for the degradation was not explored.

The form (89) for range variate $\mathbf{y}$ was also encountered in the considerations for the first-order EDF and PDF of the maximum variate; therefore, all the earlier results for SP equations and PDs of the EDF and PDF can be brought to bear directly on the range variate, with due consideration again given to the limitations imposed by a large value of M = N(N-1).

GRAPHICAL RESULTS

Figure 14 displays results for the CDF of range variate **y** in equation (89) for the GTE. The SPA a_e tracks the lower tail well below the capability of the simulation (1e8 trials), but underestimates the true CDF values in the central region and upper tail. The EDF SPA a_e in figure 15 is more accurate over its entire range, except at the lower tail. Finally, the PDF SPA a_e in figure 16 gives an accurate representation of both tails, but is a slight underestimate in the central region.

The corresponding results for the ETE are given in figures 17 through 19. The accuracies of the CDF, EDF, and PDF appear to be slightly better than those for the GTE above. Despite the sharp drop-off of the PDF in figure 19 at the lower limit, the SPA continues to track the decay; the near-origin threshold value is y = 0.001, for which log10(PDF) = -7.5.

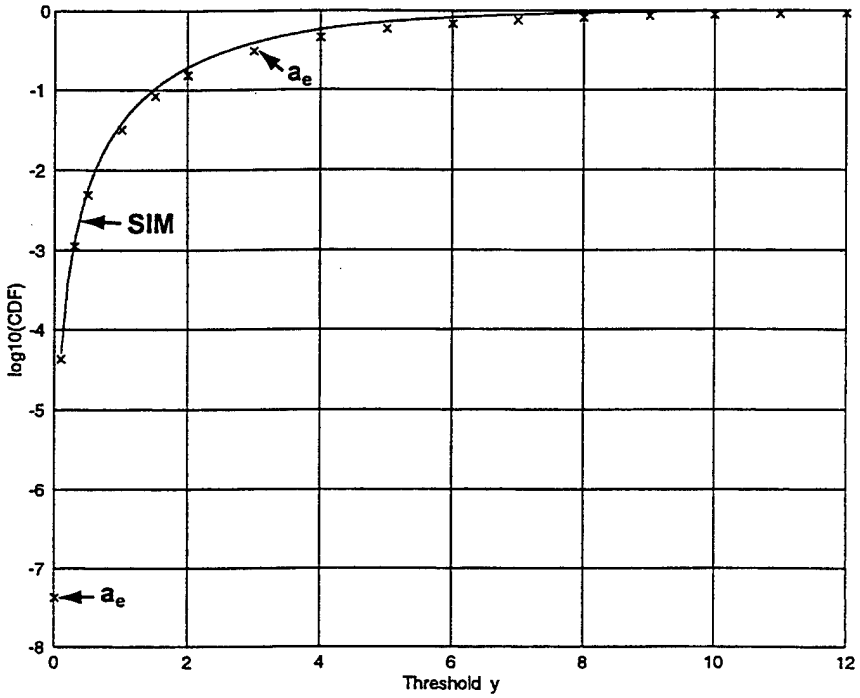

Figure 14. CDF of Range Variate for GTE

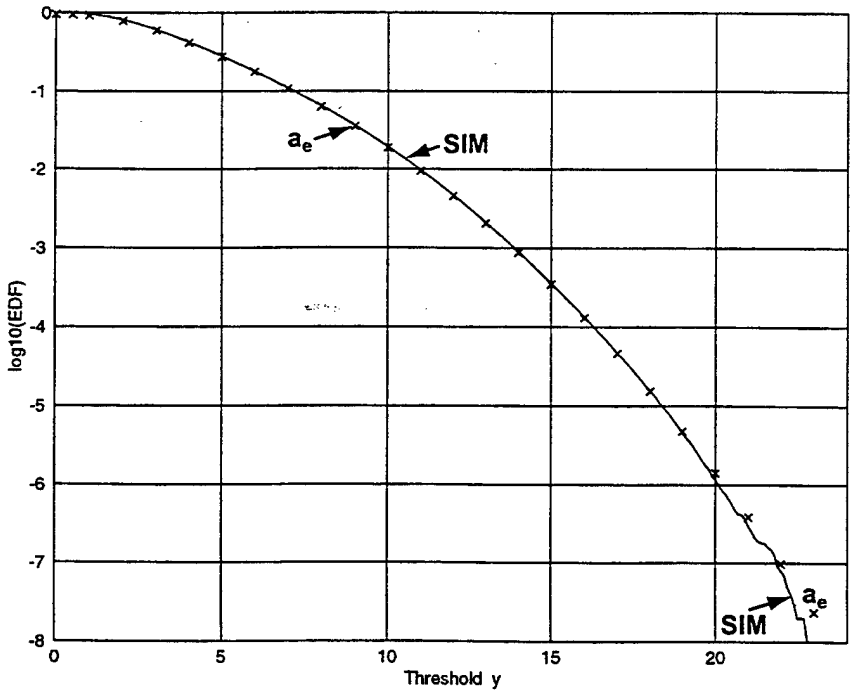

Figure 15. EDF of Range Variate for GTE

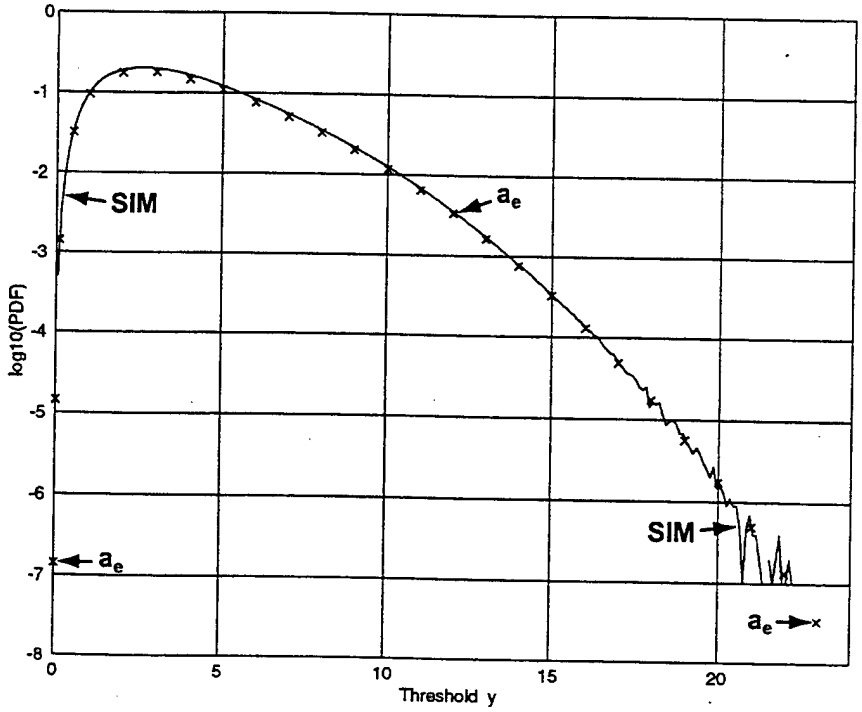

Figure 16. PDF of Range Variate for GTE

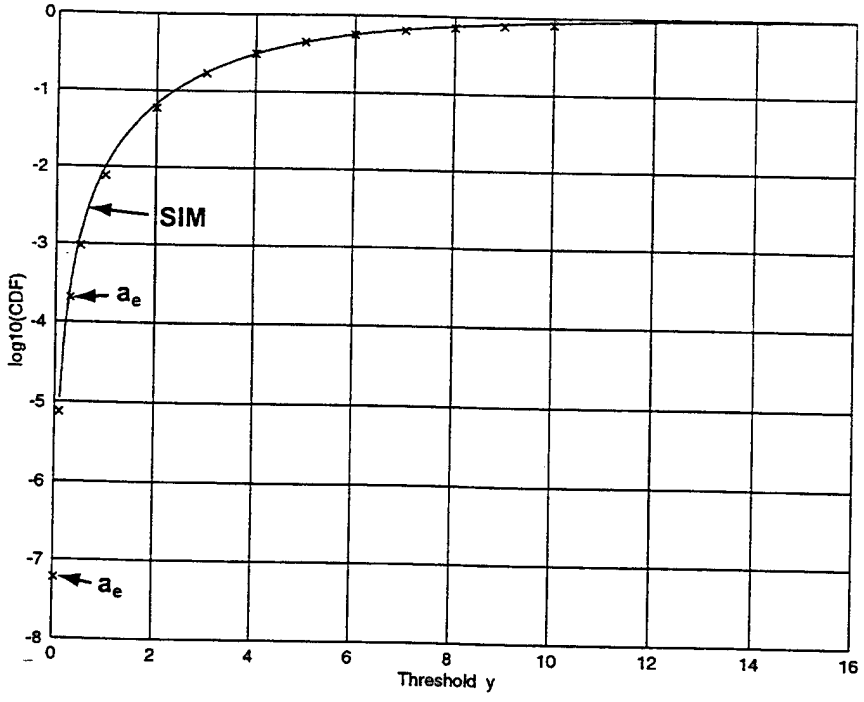

Figure 17. CDF of Range Variate for ETE

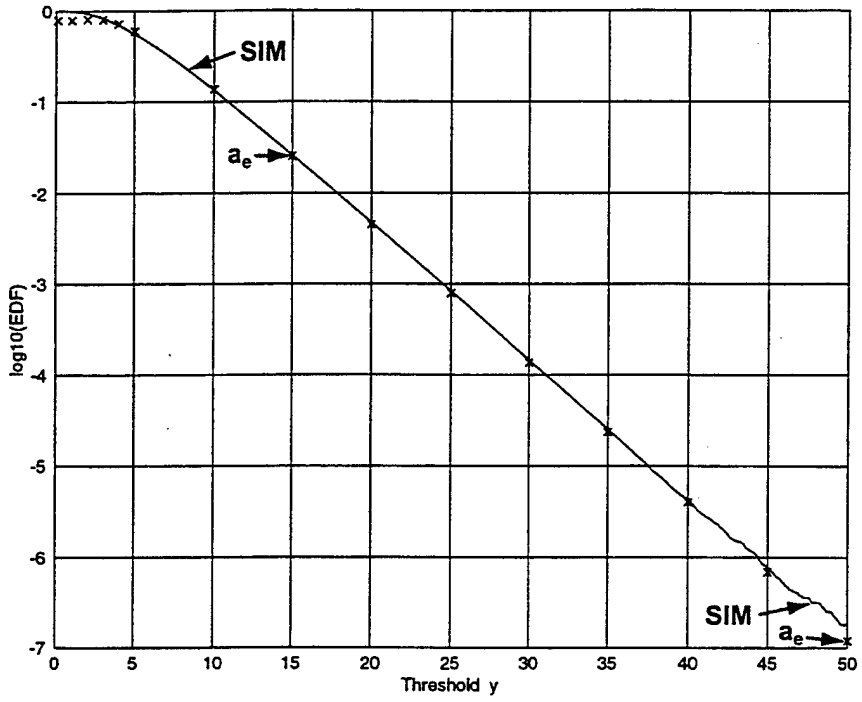

Figure 18. EDF of Range Variate for ETE

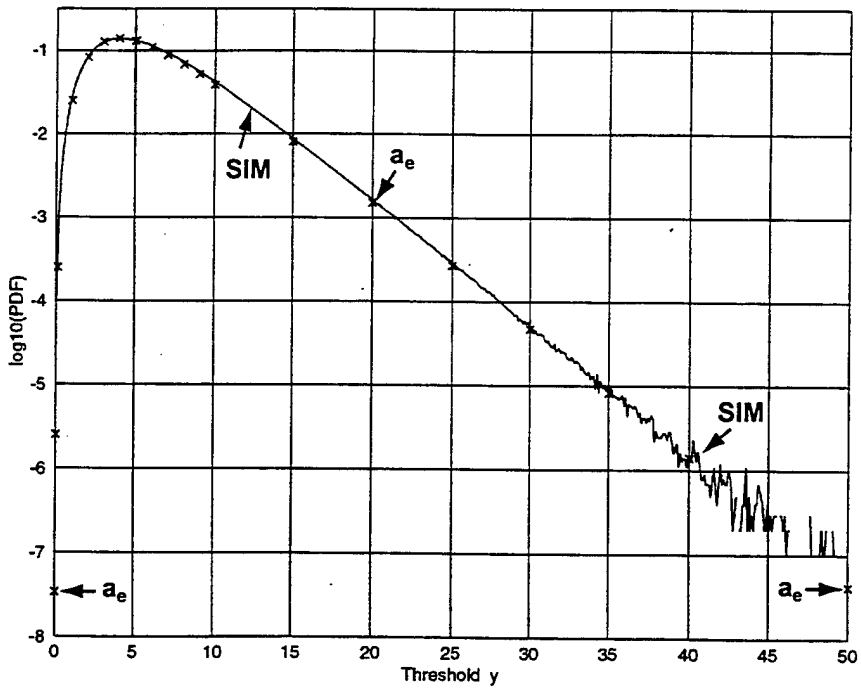

Figure 19. PDF of Range Variate for ETE

THREE ADDITIONAL PROBABILISTIC PROBLEMS

The following three problems illustrate some additional capabilities of the approach using the joint MGF in the transform domain. Outlines of the solutions are given, but no numerical results have been evaluated.

JOINT CDF OF THE TWO LARGEST RANDOM VARIABLES

Random vector $\mathbf{z} = [z_1 \cdots z_M]'$ is observed; these RVs are statistically dependent with joint MGF $\mu_z(\lambda)$. This data vector $\mathbf{z}$ is ordered into set $\mathbf{y} = [y_1 \cdots y_M]'$ where

$$y_M \leq y_{M-1} \leq \cdots \leq y_2 \leq y_1 \ . \tag{93}$$

The joint CDF of the two largest RVs, y_1 and y_2, is of interest; that is, probability

$$\Pr(y_1 < y_1,\ y_2 < y_2) \quad \text{with thresholds} \quad y_2 < y_1 \tag{94}$$

is desired for arbitrary joint MGF $\mu_z(\lambda)$.

There are two ways event (94) can occur. In the first, all the RVs $\{z_m\}$ can be less than threshold y_2. This is given by

$$\Pr(y_1 < y_2,\ y_2 < y_2) = c_z(y_2, y_2, \ldots, y_2) \ , \tag{95}$$

which is simply the joint CDF of RV $\mathbf{z}$ at common argument y_2. The second way event (94) occurs is when the m-th RV z_m lies in

the interval (y_2, y_1) while all the other RVs $\{z_m\}$ lie below threshold y_2. Since RV number m can vary from 1 to M, the total probability of this event is given by sum

$$\Pr(y_2 < y_1 < y_1,\ y_2 < y_2) = \sum_{m=1}^{M} \Pr(y_2 < z_m < y_1;\ z_n < y_2,\ n \neq m). \tag{96}$$

Reference to equation (18) reveals that nonlinear function g(u) should be selected as the form

$$g(u_1,\ldots,u_M) = \sum_{m=1}^{M} \left[U\left(u_m - y_2\right) - U\left(u_m - y_1\right)\right] \prod_{\substack{n=1 \\ n\neq m}}^{M} U\left(y_2 - u_n\right). \tag{97}$$

The corresponding gamma function is then

$$\gamma(\lambda_1,\ldots,\lambda_M) = \sum_{m=1}^{M} \frac{\exp(-\lambda_m y_2) - \exp(-\lambda_m y_1)}{\lambda_m} \prod_{\substack{n=1 \\ n\neq m}}^{M} \left\{\frac{\exp(-\lambda_n y_2)}{-\lambda_n}\right\}. \tag{98}$$

For a given value of m in the outer sum, λ_m is unrestricted but the parameters $\{\lambda_n\}$ in the inner product must satisfy $\mathrm{Re}(\lambda_n) < 0$ for all $n \neq m$. Of course, all $\{\lambda_m\}$ must always remain within the $\mathrm{ROA}(\mu_z)$ of the joint MGF $\mu_z(\lambda)$. Expression (98) can now be used in equation (18) to evaluate probability (96).

To get the CDF for the special case of the second-largest RV y_2, simply let threshold $y_1 = +\infty$ above. Then, $c_{y_2}(y_2)$ is the probability $\Pr(y_2 < y_2)$. It can be appreciated that the probability of obtaining the second-order CDF of the third-largest and seventh-largest RVs of set z would be extremely formidable due to the excessive number of cases to evaluate.

OR-ING AND POST-AVERAGING

The or-ing operation consists of taking the maximum of a set of RVs and comparing with a threshold for purposes of deciding on signal presence or absence. However, for low signal-to-noise ratios, it is frequently desirable to perform further averaging prior to the threshold comparison. This leads to consideration of the random quantity

$$y = \alpha \max(a_1,\ldots,a_A) + \beta \max(b_1,\ldots,b_B) + \psi \max(c_1,\ldots,c_C) + \cdots \tag{99}$$

where the RVs **a**, **b**, **c**,... could be statistically dependent on each other. Expression (99) can be modified into the form

$$y = \max(z_1,\ldots,z_M) \ , \tag{100}$$

where M = A B C ... The reason for this product is because any element of the RV **a** must be allowed to interact with any element of the RV **b**, etc., in equation (99). The RV **z** in equation (100) is simply a linear transformation of the RVs **a**, **b**, **c**,... and its joint MGF can be determined from the joint MGF of RVs **a**,**b**,**c**,...; however, a note of caution is in order here: dimension size M = A B C ... can get very large very quickly, being the product of the sizes of the RVs in equation (99).

The minimum of a set of RVs can be easily translated to more familiar terms by using the relation

$$\min(v_1,\ldots,v_N) = - \max(-v_1,\ldots,-v_N) \ . \tag{101}$$

RATIO OF DEPENDENT RANDOM VARIABLES

Let RV $z = [z_1 \; z_2]'$ have joint MGF $\mu_z(\alpha_1,\alpha_2)$ with ROA(μ_z). The statistics of the ratio of RVs, namely,

$$w = z_1/z_2 \; , \tag{102}$$

are of interest. In this subsection, RV z_2 is presumed to be positive; the general case of arbitrary z_2 values is treated in the appendix.

The first-order CDF of RV w is given by

$$c_w(w) = \Pr(z_1/z_2 < w) = \Pr(z_1 < w\, z_2) = \Pr(z_1 - w\, z_2 < 0) \; . \tag{103}$$

Define auxiliary RV $v = z_1 - w\, z_2$. Then,

$$c_w(w) = \Pr(v < 0) = c_v(0) = \frac{1}{i2\pi} \int_{C_1} d\lambda \; \mu_v(\lambda)/(-\lambda) \; , \tag{104}$$

which is a one-dimensional contour integral passing to the left of the origin in the complex λ-plane. The required first-order MGF of RV v is

$$\mu_v(\lambda) = E \exp(\lambda\, v) = E \exp(\lambda\, z_1 - \lambda\, w\, z_2) = \mu_z(\lambda, -w\lambda) \; , \tag{105}$$

where $(\lambda, -w\lambda) \; \varepsilon \; ROA(\mu_z)$. Substitution in equation (104) yields the first-order CDF of ratio w in the form

$$c_w(w) = \frac{1}{i2\pi} \int_{C_1} d\lambda \; \mu_z(\lambda, -w\lambda)/(-\lambda) \; . \tag{106}$$

The corresponding first-order EDF of ratio w can be found in a similar manner:

$$e_w(w) = \frac{1}{i2\pi} \int_{C_r} d\lambda \; \mu_z(\lambda, -w\lambda)/\lambda \; , \tag{107}$$

from which there follows the first-order PDF

$$p_w(w) = \frac{1}{i2\pi} \int_{C} d\lambda \; \mu_z^{(2)}(\lambda, -w\lambda) \; . \tag{108}$$

The superscript (2) denotes a partial derivative of joint MGF $\mu_z(\alpha_1,\alpha_2)$ with respect to the second argument α_2. The contour C in integral (108) need satisfy only the constraint $(\lambda, -w\lambda)$ ε ROA(μ_z) whereas contour integrals (106) and (107) have additional half-plane restrictions. Additional details about the $\Lambda(\lambda)$ function for equation (108) are found in the appendix.

If RVs z_1 and z_2 in equation (102) are quadratic and linear forms in arbitrary correlated Gaussian RVs, the required joint MGF $\mu_z(\alpha_1,\alpha_2)$ is given in reference 1, equation (23), by setting M = 2. In particular, let RV

$$z_2 = \mathbf{x}' \; C \; \mathbf{x} + v' \; \mathbf{x} + u \; , \tag{109}$$

where square matrix C is positive definite. Then, expressing

$$z_2 = (\mathbf{x} + C^{-1} \; v/2)' \; C \; (\mathbf{x} + C^{-1} \; v/2) + u - \frac{1}{4} \; v' \; C^{-1} \; v \; , \tag{110}$$

it can be seen that no matter what value random vector $\mathbf{x}$ takes on, random variable z_2 must satisfy

$$z_2 \geq u - \frac{1}{4} v' C^{-1} v \ . \qquad (111)$$

If the right-hand side of equation (111) is non-negative, then the results in equations (102) through (108) are directly applicable. If RV **x** is unable to take on the vector value $-C^{-1} v/2$, then the non-negative restriction on the right-hand side of equation (111) can be eased. The general case of arbitrary z_2 values in ratio (102) is undertaken in the appendix.

SUMMARY

A method for obtaining SPAs for some M-dimensional probabilistic problems of great practical interest has been derived and then applied to some representative examples. The accuracy of the SPAs has been verified by using a combination of simulation, asymptotic forms, and Gauss-Hermite quadrature in M dimensions. The SPA with a first-order correction term has been the model for these numerical results.

The main relation utilized is given by

$$\int du\ p_z(u)\ g(u) = \frac{1}{(i2\pi)^M} \int_C d\lambda\ \mu_z(\lambda)\ \gamma(\lambda)\ , \qquad (112)$$

where joint PDF $p_z(u)$ and joint MGF $\mu_z(\lambda)$ are a Laplace transform pair, as are functions $g(u)$ and $\gamma(\lambda)$. M-dimensional relation (112) is exact; however, numerical evaluation of either side requires adoption of an approximation technique. In particular, the approach adopted is to utilize SPAs with a correction term; this, in turn, requires that fourth-order partial derivatives be evaluated for the joint CGF $\chi_z(\lambda) = \ln \mu_z(\lambda)$.

For overlapping positive functions $p_z(u)$ and $g(u)$, there is only one SP on the real axes in the common ROA of the product $\mu_z(\lambda)\ \gamma(\lambda)$ in the transform domain. This has been the experience in the numerical results here. However, if $p_z(u)$ or $g(u)$ are not positive, the SPs can lie anywhere in the complex λ planes.

All the $g(u) = g(u_1,\ldots,u_M)$ functions considered here were separable in their arguments $(u_1,\ldots,u_M)$, except for one two-dimensional case. This separability enables the use of one-dimensional Laplace transform tables in order to obtain the corresponding $\gamma(\lambda)$ function. If g(u) is not separable, determination of $\gamma(\lambda)$ can be extremely difficult and a definite impediment to progress.

Considerable storage and execution time can be required for some of these M-dimensional problems. For example, the determination of the first-order PDF of the maximum of a set of M dependent RVs requires that M M-dimensional integrals and SPs be evaluated. Also, some combinatorial problems quickly encounter large increases in the number of alternatives that must be considered for an exact representation of the probability under investigation. These limitations serve to restrict the use of the technique in practice.

APPENDIX — STATISTICS OF RATIO

The statistics of ratio $w = z_1/z_2$, as in equation (102), are of interest, where $\mu_z(\alpha_1,\alpha_2)$ is the joint MGF of RV $z = [z_1\ z_2]'$. However, now, the denominator RV z_2 can be positive or negative. The first-order CDF of ratio w is

$$c_w(w) = \Pr(z_1 < w\ z_2,\ z_2 > 0) + \Pr(z_1 > w\ z_2,\ z_2 < 0) =$$

$$= \Pr(v < 0,\ z_2 > 0) + \Pr(v > 0,\ z_2 < 0) =$$

$$= \frac{1}{(i2\pi)^2} \int_{C_l} d\lambda_1 \int_{C_r} d\lambda_2\ \mu_{vz_2}(\lambda_1,\lambda_2)/(-\lambda_1\lambda_2) +$$

$$+ \frac{1}{(i2\pi)^2} \int_{C_r} d\lambda_1 \int_{C_l} d\lambda_2\ \mu_{vz_2}(\lambda_1,\lambda_2)/(-\lambda_1\lambda_2)\ . \qquad \text{(A-1)}$$

The RV $v = z_1 - w\ z_2$, as in equation (104). The required joint MGF in equation (A-1) is given by

$$\mu_{vz_2}(\lambda_1,\lambda_2) = E\ \exp\left[\lambda_1\left(z_1 - w\ z_2\right) + \lambda_2\ z_2\right] = \mu_z(\lambda_1,\lambda_2-w\lambda_1) \qquad \text{(A-2)}$$

in terms of the joint MGF $\mu_z(\alpha_1,\alpha_2)$ of RV z. Of course, it is required that argument $(\lambda_1,\lambda_2-w\lambda_1)\ \varepsilon\ ROA(\mu_z)$. Equation (A-2) can be substituted into equation (A-1) to get first-order CDF

$$c_w(w) = \frac{1}{(i2\pi)^2} \int_{C_l} d\lambda_1 \int_{C_r} d\lambda_2\ \mu_z(\lambda_1,\lambda_2-w\lambda_1)/(-\lambda_1\lambda_2) +$$

$$+ \frac{1}{(i2\pi)^2} \int_{C_r} d\lambda_1 \int_{C_l} d\lambda_2\ \mu_z(\lambda_1,\lambda_2-w\lambda_1)/(-\lambda_1\lambda_2)\ . \qquad \text{(A-3)}$$

Thus, two two-dimensional integrals need to be evaluated in order to get CDF $c_w(w)$ of the ratio $w = z_1/z_2$; equation (A-3) is the main result of this appendix. The Λ function of equation (48) is

$$\Lambda(\lambda_1,\lambda_2) = \chi_z(\lambda_1,\lambda_2-w\lambda_1) - \ln(-\lambda_1\lambda_2) \qquad (A-4)$$

for $(\lambda_1,\lambda_2-w\lambda_1) \varepsilon \text{ ROA}(\mu_z)$.

If RV z_2 is always positive, then joint PDF $p_z(z_1,z_2) = 0$ for argument $z_2 < 0$. Then, joint MGF

$$\mu_z(\lambda_1,\lambda_2) = \int_{-\infty}^{\infty} dz_1 \exp(\lambda_1 z_1) \int_0^{\infty} dz_2 \exp(\lambda_2 z_2)\, p_z(z_1,z_2) \qquad (A-5)$$

tends to zero as $\text{Re}(\lambda_2) \to -\infty$. Then, by moving the two λ_2 contours in equation (A-3) toward $-\infty$, there follows, respectively,

$$\frac{1}{i2\pi} \int_{C_r} d\lambda_2 \frac{\mu_z(\lambda_1,\lambda_2-w\lambda_1)}{\lambda_2} = \mu_z(\lambda_1, -w\lambda_1) \qquad (A-6)$$

and

$$\frac{1}{i2\pi} \int_{C_1} d\lambda_2 \frac{\mu_z(\lambda_1,\lambda_2-w\lambda_1)}{-\lambda_2} = 0 \ . \qquad (A-7)$$

Therefore, equation (A-3) reduces to

$$c_w(w) = \frac{1}{i2\pi} \int_{C_1} d\lambda_1 \frac{\mu_z(\lambda_1, -w\lambda_1)}{-\lambda_1} \ , \qquad (A-8)$$

in agreement with equation (106).

As an application of this approach by means of joint MGF functions, the first-order PDF of Student's ratio will be derived. Let g and $(g_1,\ldots,g_n)$ be independent, identically distributed Gaussian RVs of zero mean and unit variance (without loss of generality). Also, let

$$s = \left(\frac{g_1^2 + \cdots + g_n^2}{n}\right)^{\frac{1}{2}} . \tag{A-9}$$

Student's ratio is

$$w = \frac{g}{s} = \frac{g\ s}{s^2} \equiv \frac{z_1}{z_2} . \tag{A-10}$$

RV z_2 is obviously positive, thereby allowing use of equation (108). The joint MGF of RV $z = [z_1\ z_2]'$ is

$$\mu_z(\lambda_1,\lambda_2) = E_z \exp(\lambda_1 z_1 + \lambda_2 z_2) = E_{sg} \exp\left(\lambda_1\ g\ s + \lambda_2\ s^2\right) =$$

$$= E_s\left[\exp\left(\lambda_2 s^2\right) \exp\left(\tfrac{1}{2}\lambda_1^2 s^2\right)\right] = \left[1 - \left(2\lambda_2+\lambda_1^2\right)/n\right]^{-\frac{1}{2}n} \tag{A-11}$$

for $\mathrm{Re}(2\lambda_2 + \lambda_1^2) < n$. A partial derivative with respect to λ_2 yields

$$\mu_z^{(2)}(\lambda_1,\lambda_2) = \left[1 - \left(2\lambda_2+\lambda_1^2\right)/n\right]^{-\frac{1}{2}n-1} . \tag{A-12}$$

Therefore,

$$\mu_z^{(2)}(\lambda,\ -w\lambda) = \left[1 + \left(2w\lambda-\lambda^2\right)/n\right]^{-\frac{1}{2}n-1} \quad \text{for } \mathrm{Re}\left(\lambda^2-2w\lambda\right) < n . \tag{A-13}$$

At this point, make the change of variable $\lambda = w + iu$, where u is real. Then, equations (108) and (A-13) yield, for all w,u,

$$p_w(w) = \frac{1}{i2\pi} \int_C d\lambda \left[1 + (2w\lambda - \lambda^2)/n\right]^{-\frac{1}{2}n-1} = \tag{A-14}$$

$$= \frac{1}{2\pi} \int_{-\infty}^{\infty} du \left[1 + (w^2 + u^2)/n\right]^{-\frac{1}{2}n-1} =$$

$$= \frac{\Gamma(\frac{1}{2}(n+1))}{(n\pi)^{\frac{1}{2}}\, \Gamma(\frac{1}{2}n)\, [1 + w^2/n]^{\frac{1}{2}(n+1)}} \quad \text{for all } w \, . \tag{A-15}$$

The last integral on u was determined from reference 4, equation 3.241 4. Exact result (A-15) is Student's PDF for ratio w in equations (A-9) and (A-10).

Alternatively, the SPA to equation (A-14) is obtained by observing that

$$\Lambda(\lambda) = -(\tfrac{1}{2}n+1)\, \ln\left[1 + (2w\lambda - \lambda^2)/n\right] \, ,$$

$$\frac{d\Lambda(\lambda)}{d\lambda} = \frac{(n+2)(\lambda - w)}{n + 2w\lambda - \lambda^2} \, , \tag{A-16}$$

and

$$\frac{d^2\Lambda(\lambda)}{d\lambda^2} = (n+2)\, \frac{n + w^2 + (\lambda - w)^2}{\left[n + w^2 - (\lambda - w)^2\right]^2} \, . \tag{A-17}$$

The real SP is obtained from equation (A-16) as $\hat{\lambda} = w$, for which $\hat{\lambda}^2 - 2w\hat{\lambda} = -w^2 < n$, as required in equation (A-13). Then, equation (A-17) yields $\Lambda_2 = (n+2)/(n+w^2)$ at the SP $\hat{\lambda} = w$, while equation (55) yields SPA

$$a_0 = \left(\frac{n}{2\pi(n+2)}\right)^{\frac{1}{2}} \Big/ \left[1 + w^2/n\right]^{\frac{1}{2}(n+1)} \quad \text{for all } w \ . \tag{A-18}$$

This SPA a_0 has precisely the same variation with argument w as does exact result $p_w(w)$ in equation (A-15); however, the ratio $a_0/p_w(w)$ starts at $(\pi/6)^{\frac{1}{2}} = 0.7236$ for n = 1 and increases towards 1 as n increases. The first-order corrected SPA a_e is $a_0 \exp(0.75/(n+2))$, which is 0.9291 of $p_w(w)$ in equation (A-15) for n = 1.

In general, the $\Lambda(\lambda)$ function of equation (108) is

$$\Lambda(\lambda) = \ln \mu_2(\lambda, -w\lambda) \ , \tag{A-19}$$

where a subscript notation for PDs has been adopted. But, since $\mu(\alpha,\beta) = \exp[\chi(\alpha,\beta)]$, there follows

$$\mu_2(\alpha,\beta) = \mu(\alpha,\beta)\ \chi_2(\alpha,\beta) \equiv \mu(\alpha,\beta)\ \phi(\alpha,\beta) \ , \tag{A-20}$$

leading to

$$\Lambda(\lambda) = \chi(\lambda, -w\lambda) + \ln \phi(\lambda, -w\lambda) \equiv \chi + \ln \phi \ . \tag{A-21}$$

Therefore,

$$\Lambda'(\lambda) = \chi_1 - w\ \chi_2 + (\phi_1 - w\ \phi_2)/\phi \tag{A-22}$$

and

$$\Lambda''(\lambda) = \chi_{11} - 2\ w\ \chi_{12} + w^2\ \chi_{22} +$$

$$+ (\phi_{11} - 2\ w\ \phi_{12} + w^2\ \phi_{22})/\phi - (\phi_1 - w\ \phi_2)^2/\phi^2 \ . \tag{A-23}$$

Since $\phi = \phi(\lambda, -w\lambda) = \chi_2(\lambda, -w\lambda)$, the terms in equations (A-22) and (A-23) are explicitly

$$\phi_1 = \chi_{12} , \quad \phi_2 = -w\, \chi_{22} ,$$

and

$$\phi_{11} = \chi_{211} , \quad \phi_{12} = -w\, \chi_{221} , \quad \phi_{22} = w^2\, \chi_{222} . \qquad \text{(A-24)}$$

This information is sufficient to locate the SP of $\Lambda(\lambda)$ in equation (A-19) and determine SPA a_0 to equation (108).

REFERENCES

1. A. H. Nuttall, "Saddlepoint Approximation and First-Order Correction Term to the Joint Probability Density Function of M Quadratic and Linear Forms in K Gaussian Random Variables with Arbitrary Means and Covariances," NUWC-NPT Technical Report 11,262, Naval Undersea Warfare Center Division, Newport, RI, 12 December 2000.

2. N. Reid, "Saddlepoint Methods and Statistical Inference", **Statistical Science**, Volume 3, Number 2, pages 213 - 238, 1988.

3. P. M. McCullagh, **Tensor Methods in Statistics**, Chapman and Hall, England, 1987.

4. I. S. Gradshteyn and I. M. Ryzhik, **Table of Integrals, Series, and Products**, Academic Press, Inc., New York, NY, 1980.

INITIAL DISTRIBUTION LIST

Addressee	No. of Copies
Center for Naval Analyses, VA	1
Coast Guard Academy, CT	
J. Wolcin	1
Commander Submarine Force, U.S. Pacific Fleet, HI	
W. Mosa, CSP N72	1
Defense Technical Information Center	2
Griffiss Air Force Base, NY	
Documents Library	1
J. Michels	1
Hanscom Air Force Base, MA	
M. Rangaswamy	1
National Radio Astronomy Observatory, VA	
F. Schwab	1
National Security Agency, MD	
J. Maar	1
National Technical Information Service, VA	10
Naval Environmental Prediction Research Facility, CA	1
Naval Intelligence Command, DC	1
Naval Oceanographic and Atmospheric Research Laboratory, MS	
E. Franchi	1
R. Wagstaff	1
Naval Oceanographic Office, MS	1
Naval Personnel Research and Development Center, CA	1
Naval Postgraduate School, CA	
Superintendent	1
C. Therrien	1
Naval Research Laboratory, DC	
W. Gabriel	1
E. Wald	1
Naval Surface Warfare Center, FL	
E. Linsenmeyer	1
D. Skinner	1
Naval Surface Warfare Center, VA	
J. Gray	1
Naval Technical Intelligence Center, DC	
Commanding Officer	1
D. Rothenberger	1
Naval Undersea Warfare Center, FL	
Officer in Charge	1
Naval Weapons Center, CA	1
Office of the Chief of Naval Research, VA	
ONR 321 (D. Johnson)	1
ONR 321US (J. Tague)	1
ONR 322 (R. Tipper)	1
ONR 334 (P. Abraham)	1

INITIAL DISTRIBUTION LIST (Cont'd)

Addressee	No. of Copies
Office of Naval Research	
ONR 31 (R. R. Junker)	1
ONR 311 (A. M. van Tilborg)	1
ONR 312 (M. N. Yoder)	1
ONR 313 (N. L. Gerr)	1
ONR 32 (S. E. Ramberg	1
ONR 321 (F. Herr)	1
ONR 33 (S. G. Lekoudis)	1
ONR 334 (A. J. Tucker)	1
ONR 342 (W. S. Vaughan)	1
ONR 343 (R. Cole)	1
ONR 362 (M. Sponder)	1
Program Executive Office, Undersea Warfare (ASTO), VA	
J. Thompson, A. Hommel, R. Zarnich	3
U.S. Air Force, Maxwell Air Force Base, AL	
Air University Library	1
Vandenberg Air Force Base, CA	
CAPT R. Leonard	1
Brown University, RI	
Documents Library	1
Catholic University of America, DC	
J. McCoy	1
Drexel University, PA	
S. Kesler	1
Duke University, NC	
J. Krolik	1
Harvard University, MA	
Gordon McKay Library	1
Johns Hopkins University, Applied Physics Laboratory, MD	
H. M. South	1
T. N. Stewart	1
Lawrence Livermore National Laboratory, CA	
L. Ng	1
Los Alamos National Laboratory, NM	1
Marine Biological Laboratory, MA	
Library	1
Massachusetts Institute of Technology, MA	
Barker Engineering Library	1
Massachusetts Institute of Technology, Lincoln Laboratory, MA	
V. Premus	1
J. Ward	1
Pennsylvania State University, Applied Research Laboratory, PA	
R. Hettche	1
E. Liszka	1
F. Symons	1
Princeton University, NJ	
S. Schwartz	1
Rutgers University, NJ	
S. Orfanidis	1

INITIAL DISTRIBUTION LIST (Cont'd)

Addressee	No. of Copies
San Diego State University, CA	
F. Harris	1
Scripps Institution of Oceanography, Marine Physical Laboratory, CA	
Director	1
Syracuse University, NY	
D. Weiner	1
Engineering Societies Information Center, Kansas City, MO	
Linda Hall Library-East	1
University of Colorado, CO	
L. Scharf	1
University of Connecticut, CT	
Wilbur Cross Library	1
C. Knapp	1
P. Willett	1
University of Florida, FL	
D. Childers	1
University of Hartford	
Science and Engineering Library	1
University of Illinois, IL	
D. Jones	1
University of Illinois at Chicago, IL	
A. Nehorai	1
University of Massachusetts, MA	
C. Chen	1
University of Massachusetts Dartmouth, MA	
J. Buck	1
University of Michigan, MI	
Communications and Signal Processing Laboratory	1
W. Williams	1
University of Minnesota, MN	
M. Kaveh	1
University of Rhode Island, RI	
Library	1
G. Boudreaux-Bartels	1
S. Kay	1
D. Tufts	1
University of Rochester, NY	
E. Titlebaum	1
University of Southern California, CA	
W. Lindsey	1
A. Polydoros	1
University of Texas, TX	
Applied Research Laboratory	1
C. Penrod	1
University of Toronto	
N. Reid	1
University of Washington, WA	
Applied Physics Laboratory	1
D. Lytle	1
J. Ritcey	1
R. Spindel	1

INITIAL DISTRIBUTION LIST (Cont'd)

Addressee	No. of Copies
Villanova University, PA	
M. Amin	1
Woods Hole Oceanographic Institution, MA	
Director	1
T. Stanton	1
Yale University, CT	
Kline Science Library	1
P. Schultheiss	1
Analysis and Technology, CT	
Library	1
Analysis and Technology, VA	
D. Clark	1
Atlantic Aerospace Electronics Corp.	
R. Stahl	1
Bell Communications Research, NJ	
D. Sunday	1
Berkeley Research, CA	
S. McDonald	1
Bolt, Beranek, and Newman, CT	
P. Cable	1
Bolt, Beranek, and Newman, MA	
H. Gish	1
DSR, Inc., VA	
M. Bozek-Kuzmicki	1
EG&G Services, CT	
J. Pratt	1
Engineering Technology Center	
D. Lerro	1
General Electric, NJ	
H. Urkowitz	1
Harris Scientific Services, NY	
B. Harris	1
Hughes Defense Communications, IN	
R. Kenefic	1
Kildare Corporation, CT	
R. Mellen	1
Lincom Corporation, MA	
T. Schonhoff	1
Lockheed Martin, Undersea Systems, VA	
M. Flicker	1
Lockheed Martin, Ocean Sensor Systems, NY	
R. Schumacher	1
Marconi Aerospace Defense Systems, TX	
R. D. Wallace	1
MITRE Corporation, VA	
S. Pawlukiewicz	1
R. Bethel	1
Neural Technology, Inc., SC	
E. A. Tagliarini	1
Orincon Corporation, VA	
H. Cox	1

INITIAL DISTRIBUTION LIST (Cont'd)

Addressee	No. of Copies
Prometheus, RI	
M. Barrett	1
J. Byrnes	1
Raytheon, RI	
R. Conner	1
S. Reese	1
Schlumberger-Doll Research, CT	
R. Shenoy	1
Science Applications International Corporation, CA	
C. Katz	1
Science Applications International Corporation, VA	
P. Mikhalevsky	1
Toyon Research, CA	
M. Van Blaricum	1
Tracor, TX	
T. Leih	1
Westinghouse Electric, Annapolis, MD	
H. Newman	1
Westinghouse Electric, Baltimore, MD	
R. Park	1
K. Harvel, Austin, TX	1